



**ΠΟΛΥΤΕΧΝΕΙΟ ΚΡΗΤΗΣ**  
TECHNICAL UNIVERSITY OF CRETE

---

# Towards Vaccination Control Strategy Against COVID-19 for Optimal Resource Distribution Among Different Age Groups

---

*Author:*

Katsaras Stavros–Rafail

*Thesis Committee:*

Bekiaris–Liberis Nikolaos (Supervisor)

Ellinas Demosthenes

Hristopulos Dionissios

*Technical University of Crete*  
*School of Electrical and Computer Engineering*

July 2021

# Table of Contents

<b>Table of Contents</b>	<b>i</b>
<b>Acknowledgements</b>	<b>iii</b>
<b>Abstract</b>	<b>iv</b>
<b>1 Epidemiological Models</b>	<b>1</b>
1.1 Introduction . . . . .	1
1.1.1 Compartmental Models . . . . .	2
1.2 Model Design for COVID-19 Disease Dynamics . . . . .	4
1.2.1 Proposed Model without Control . . . . .	6
1.2.2 Proposed Model with Control . . . . .	9
<b>2 System Output and Measurements</b>	<b>11</b>
2.1 Introduction . . . . .	11
2.2 Collection of Data . . . . .	12
2.3 System Outputs . . . . .	12
2.4 Data Processing . . . . .	14
2.4.1 Estimation of the True Number of COVID-19 Cases . . . . .	15
2.4.2 Processing of the Vaccination Data . . . . .	16
<b>3 Parameter Specification</b>	<b>17</b>
3.1 Introduction . . . . .	17
3.2 System Identification . . . . .	17
3.2.1 Defining the Initial System States . . . . .	19
3.2.2 Estimating the System Parameters . . . . .	19

<b>4</b>	<b>Results And Discussion</b>	<b>21</b>
4.1	Estimation of the True Number of COVID-19 Cases . . . . .	21
4.1.1	Basic Reproduction Number ( $R_0$ ) and $R_t$ . . . . .	22
4.2	Parameter Specification . . . . .	23
4.2.1	Vaccination Parameters . . . . .	23
4.2.2	Time-Varying System Parameters . . . . .	24
4.3	Fitting the System Outputs to the Measurements . . . . .	32
4.3.1	System Outputs for Cases . . . . .	32
4.3.2	System Outputs for Deaths . . . . .	34
4.3.3	System Outputs for Recovered Individuals . . . . .	37
4.3.4	System Outputs for Vaccinated Individuals . . . . .	38
4.4	Investigating the Relation between NPI and fatality rates . . . . .	45
<b>5</b>	<b>Pontryagin's Minimum Principle</b>	<b>48</b>
5.1	Introduction . . . . .	48
5.2	Theoretical Background for Pontryagin's Minimum Principle . . . . .	49
5.3	Application of Pontryagin's Principle in the System with Control . . . . .	53
5.3.1	Formulation of the Optimal Control Problem . . . . .	53
5.3.2	Existence of Optimal Control . . . . .	53
5.3.3	Characterizing the Optimal Controller . . . . .	54
<b>6</b>	<b>Conclusions And Future Work</b>	<b>63</b>
6.1	Summary . . . . .	63
6.2	Future Work . . . . .	64
	<b>Bibliography</b>	<b>65</b>

# Acknowledgements

A challenging yet fulfilling journey of undergraduate studies is drawing to a close. During my time as a student I was able to earn powerful theoretical background and valuable hands-on experience regarding all research fields that comprise the subject of ECE. First of all, I would like to express my sincere gratitude to the personnel of the school, who are significantly involved in providing a strong foundation of knowledge to every student and contributing to the development of research in all fields.

I would also like to express my gratitude to each member of the Thesis Committee for taking the time to assess the work that has been conducted in this thesis statement; it has been an honor for me to have collaborated with the Committee. I would like to thank professor Bekiaris–Limperis Nikolaos, the supervisor of this thesis, for his valuable guidance throughout this work, his inspiration, as well as for his continuous support.

Last, but not least, I would also like to thank my family for making it possible for me to study and achieve my dreams, despite the hardships. Without my family’s lifetime support and endeavors, I wouldn’t have made it this far. The completion of my undergraduate studies marks the beginning of a whole new era for me, in which I can finally contribute to the society by using the knowledge that I have obtained.

*Katsaras Stavros–Rafail,  
June 2021*

# Abstract

The rapid dissemination of the COVID-19 pandemic in recent times has turned the focus upon developing strategies for eradicating the COVID-19 disease. As development of vaccinations against SARS-CoV-2 virus has proven to be useful for the immunization and prevention of severe cases, it is important to employ optimal control policies regarding inoculation of a population while taking into consideration factors such as the available vaccine resources, the death counts and attaining herd immunity.

In this work, an age-structured compartmental epidemiological model is proposed in order to model the dynamics of COVID-19. The model is then used to describe the dissemination of the disease in Greece based on available data using system identification techniques and a-priori knowledge of the disease behavior. The available data are processed to estimate the true number of infections and to best suit the model. The results are then presented for the data processing, the specification of the system parameters and the fitting of the system outputs to the data. Finally, preliminary work on the optimal vaccination control strategy based on Pontryagin's Minimum Principle is presented for a controller which drives the system to herd immunity while minimizing the vaccine resource utilization and the number of deaths in the population.

# Chapter 1

## Epidemiological Models

### 1.1 Introduction

Novel coronavirus disease (COVID-19) has imposed an intractable challenge upon communities because of its highly contagious nature and its characteristics regarding transmission which are not yet fully understood.

This has given rise to questions regarding the prediction of the dynamics of this disease in a population, as well as the employment of control policies either through non-pharmaceutical interventions or vaccination.

Several models have been proposed for modeling disease dynamics and developing optimal control policies. The oldest reference to an epidemic model in the literature dates back to the 16th century. The model was proposed by Bernoulli, D. as an attempt to model the spread of smallpox. The following types of epidemiological models have prevailed up to present time:

- Compartmental Models
  - Stochastic Models
  - Deterministic Models
- Epidemiological Agent-Based Models

Agent-Based Models (ABMs) model the behavior of individuals in a population by utilizing autonomous decision-making entities called ‘agents’ [1]. The agents’ decisions are probabilistic, therefore ABMs are inherently stochastic models. ABMs are not governed by mathematical equations, such as Ordinary or

Partial Differential Equations (ODEs/PDEs). This renders ABMs unsuitable for use in the field of Control Systems. [2, 3]

In the following paragraph, Compartmental Models are discussed.

### 1.1.1 Compartmental Models

Compartmental models comprise the dominant type of epidemiological models. These include well-celebrated models such as SIR, SEIR, etc., and some variations of these models adapted to specific aspects regarding our knowledge of the characteristics of the disease (eg. latent period) or aspects that *inherently* affect social interactions and thus affecting spread (such as isolation through hospitalization). The concept of dividing the population in groups (termed ‘compartments’) of specific interest in the dissemination of a disease was introduced in 1926 by Kermack, W.O. and McKendrick, A.G., who developed the SIR model [4]. Among the works that were published in the early 20th-century, the SIR model proposed by Kermack, W.O. and McKendrick, A.G. was able to adequately describe various disease outbreaks at that time.

Compartmental models are further divided into deterministic and stochastic models. Stochastic Epidemic Models involve the use of stochastic processes in order to account for uncertainty in the parameters. The SIR model proposed by Kermack, W.O. and McKendrick, A.G. is an example of a deterministic compartmental model, since it does not model any uncertainty in the parameters. Common processes used in compartmental epidemiological systems are Markov chains (in the discrete-time case) and Markov processes (in the continuous-time case). Markov chains/processes can easily be applied to compartmental modeling due to the inherent characteristic of transitions among compartments in compartmental models. [5, 6]

Various models have been proposed for modelling the epidemic dynamics of COVID-19 disease and control of such epidemiological systems [Table 1.1]. These models generally do not rely upon precise biological laws, but often on observations on the effects of the disease in a given population.

A summary of the SIR [4] compartmental model is given in [Table 1.1]. Variants of the SIR include the SIRD [7] model, which takes into consideration the mortality of the disease, the SIHRD [8][9] model, which also describes the disease dynamics upon the hospitalized population.

Moreover, SEIR model accounts for the effect of the disease dynamics on the early stages of the infection. The Exposed (E) compartment is typically used for integrating the effects of the disease latency period for diseases that are not contagious immediately after infection. However, for diseases where this is not the case, the exposed (E) compartment can also be used for describing the incubation period.

The SIR model accounts for permanent immunity once an infected individual recovers from the disease. This can be a reasonable assumption for diseases like measles, rubella, etc. However, for many diseases, the acquired immunity may be short-term, lasting for several months (such as the flu, the novel coronavirus disease, etc.), or several decades (such as the smallpox). The SIRS and SEIRS [10] models consider short-term immunity, therefore are suitable for modelling the dynamics of such diseases.

The SLIAR/SEIAR [11] model describe the effects of the symptomatic and asymptomatic population. This can be particularly useful, for example, when the asymptomatic population can spread the disease with a different rate the symptomatic (who may practice self-isolation or be hospitalized).

Furthermore, the disease dynamics may vary depending on certain characteristics of each individual. For example, it has been observed that the novel coronavirus disease has a higher mortality rate among male individuals [12], individuals with comorbidity and underlying diseases [13] or elderly individuals [14]. Moreover, studying how the disease spread evolves among individuals based on social factors is of substantial significance in order to acquire a more solid understanding of the social and economic impact of the disease upon the population.

Compartmental models, despite their simple and intuitive structure, impose an unrealistic assumption of homogeneity of susceptible and infectious individuals in the population. This assumption might be acceptable in small populations, however in larger populations (e.g. considering the population of a country) it can lead to wrong dynamical evolution of the disease in the model.

## Network-based Compartmental Models

The oversimplifying assumption of homogeneity in the population can be dealt with (for finite-dimensional state vectors) by introducing groups of the population in the model based on a specific attribute of the individuals and by modeling the interactions among these groups. Individuals can be differentiated by attributes such as:

- geolocation,
- age,
- gender,
- underlying medical conditions, e.g. heart disease, obesity, etc.

Depending on the number of groups that the population is divided into, homogeneity becomes less effective on the dynamics.

## 1.2 Model Design for COVID-19 Disease Dynamics

Choosing and designing an appropriate model for forecasting the epidemic behavior of COVID-19 in a given population should satisfy the following criteria:

- *concisely* describe the different *groups* of the population which are of substantial importance when studying the disease influence upon these groups,
- *adequately* take into consideration social interactions among the population.
- a control strategy can *effectively* be applied and its effect can be reflected on the system equations, and
- the model should *flexibly* adapt to given data sets when parameter identification is considered.

In this work, two-dose vaccination is considered as most of the vaccines approved so far for COVID-19 require a two-dose administration.

Model	Equation Count	Description of the System States	Application	References
SIR	3	The SIR model comprises three (3) state variables: <b>the susceptible (S)</b> population, indicating the population which is vulnerable to the disease, <b>the infectious (I)</b> population which have contracted the disease and can further transmit it, and <b>the removed (R)</b> population, which has either recovered from the disease (acquiring permanent immunity) or have been removed from the population (due to migration or death).	●	[4], [15], [16], [17], [8]
SIRD	4	The SIRD model additionally takes into consideration the <b>deceased (D)</b> in an explicit manner, either because of demography or due to the disease.	◐	[7], [18]
SIQR	4	In addition to the SIR model, SIQR takes into consideration the <b>quarantined (Q)</b> population, effectively describing the number of the diagnosed cases.	◑	[19], [20]
SIHRD	5	Similar to SIQR, the SIHRD takes into consideration the <b>hospitalized (H)</b> population, which does not transmit the disease (eg. due to hospital protocol). Moreover, SIHRD considers the fraction of the population that is deceased (D).	◑	[8], [9]
SEIR	4	In addition to the SIR model, SEIR also accounts for the latent or incubation period of the population that is <b>exposed (E)</b> to the disease. Alternatively, the E compartment can be considered to describe the pre-symptomatic population.	●	[21], [22], [23]
SEIRS	4	The SEIRS model is a slight modification the SEIR model, in that the acquired immunity is temporary.	●	[10], [24], [25]
SEIHRD	6	Similar to SIHRD, SEIHRD also includes the <b>exposed (E)</b> population.	◑	[26]
MSEIR	5	In addition to the SEIR model, the MSEIR model also takes into account the <b>maternal (M)</b> immunity of the newborn population, eg. as maternal antibodies are transmitted during pregnancy.	○	[27]
SUQC	4	The SUQC model comprises the <b>susceptible (S)</b> population, the <b>unquarantined (U)</b> infectious population, the <b>quarantined (Q)</b> infectious population either through self-isolation or hospitalization, as well as the <b>officially confirmed (C)</b> cases.	◑	[28], [29]
SLIAR (SEIAR)	5	Similar to SEIR, the SLIAR (SEIAR) model considers the population that is <b>exposed (S)</b> to the disease. Moreover, this model makes a distinction between <b>symptomatic infectious (I)</b> and <b>asymptomatic infectious (A)</b> population.	◑	[11]
SIDARTHE	8	The SIDARTHE model is essentially an expansion of the infectious (I) and removed (R) compartments of the SIR model. Specifically, it comprises the <b>susceptible (S)</b> population, the <b>infectious (I)</b> asymptomatic and undiagnosed population, the <b>diagnosed (D)</b> symptomatic population, the <b>ailing (A)</b> undiagnosed but symptomatic infected population, the <b>recognized (R)</b> symptomatic and diagnosed population, the <b>threatened (T)</b> population in deteriorating condition, the <b>healed (H)</b> from the disease population and, lastly, the <b>extinct (E)</b> from the disease population.	◑	[30], [31]

**Table 1.1:** Brief overview of commonly used compartmental models in epidemiological systems modelling and control. The circular indication with the upper half part filled ● denotes a model that has been used for modelling COVID-19 dynamics, the circular indication with the lower left half part filled ◐ denotes a model that has been used for control using non-pharmaceutical interventions, while the circular indication with the lower right half part filled ◑ indicates a model that has been used for vaccination control.

### 1.2.1 Proposed Model without Control

In this study, an age-structured model is proposed which describes the spread of the disease among individuals of different age groups. This enables us to study the following aspects of the disease spread:

- study the evolution of the disease on each age group, based on the disease dynamics, and
- how each age-group influences all others through social factors, such as social contacts.

Taking the above into consideration, define the state vector of the system as  $\mathbf{x}(t) = [\mathbf{S}(t) \ \mathbf{E}(t) \ \mathbf{I}(t) \ \mathbf{R}(t) \ \mathbf{V}_+^l(t) \ \mathbf{V}_-^l(t) \ \mathbf{D}(t)]^\top$ . Then, following model is proposed:

$$\dot{\mathbf{x}}(t, \mathbf{x}(t)) := \mathbf{f}(t, \mathbf{x}(t)) = \frac{d}{dt} \begin{bmatrix} \mathbf{S}(t, \mathbf{x}(t)) \\ \mathbf{E}(t, \mathbf{x}(t)) \\ \mathbf{I}(t, \mathbf{x}(t)) \\ \mathbf{R}(t, \mathbf{x}(t)) \\ \mathbf{V}_+^l(t, \mathbf{x}(t)) \\ \mathbf{V}_-^l(t, \mathbf{x}(t)) \\ \mathbf{D}(t, \mathbf{x}(t)) \end{bmatrix} = \begin{bmatrix} \mathbf{f}_S(t, \mathbf{x}(t)) \\ \mathbf{f}_E(t, \mathbf{x}(t)) \\ \mathbf{f}_I(t, \mathbf{x}(t)) \\ \mathbf{f}_R(t, \mathbf{x}(t)) \\ \mathbf{f}_{V_+^l}^l(t, \mathbf{x}(t)) \\ \mathbf{f}_{V_-^l}^l(t, \mathbf{x}(t)) \\ \mathbf{f}_D(t, \mathbf{x}(t)) \end{bmatrix}, \quad (1.1)$$

where

$$\begin{aligned} \mathbf{S}(t, \mathbf{x}(t)) &= [S^1(t, \mathbf{x}(t)) \ S^2(t, \mathbf{x}(t)) \ S^3(t, \mathbf{x}(t)) \ S^4(t, \mathbf{x}(t))], \\ \mathbf{E}(t, \mathbf{x}(t)) &= [E^1(t, \mathbf{x}(t)) \ E^2(t, \mathbf{x}(t)) \ E^3(t, \mathbf{x}(t)) \ E^4(t, \mathbf{x}(t))], \\ \mathbf{I}(t, \mathbf{x}(t)) &= [I^1(t, \mathbf{x}(t)) \ I^2(t, \mathbf{x}(t)) \ I^3(t, \mathbf{x}(t)) \ I^4(t, \mathbf{x}(t))], \\ \mathbf{R}(t, \mathbf{x}(t)) &= [R^1(t, \mathbf{x}(t)) \ R^2(t, \mathbf{x}(t)) \ R^3(t, \mathbf{x}(t)) \ R^4(t, \mathbf{x}(t))], \\ \mathbf{V}_+^l(t, \mathbf{x}(t)) &= [V_+^{l,1}(t, \mathbf{x}(t)) \ V_+^{l,2}(t, \mathbf{x}(t)) \ V_+^{l,3}(t, \mathbf{x}(t)) \ V_+^{l,4}(t, \mathbf{x}(t))], \\ \mathbf{V}_-^l(t, \mathbf{x}(t)) &= [V_-^{l,1}(t, \mathbf{x}(t)) \ V_-^{l,2}(t, \mathbf{x}(t)) \ V_-^{l,3}(t, \mathbf{x}(t)) \ V_-^{l,4}(t, \mathbf{x}(t))], \\ \mathbf{D}(t, \mathbf{x}(t)) &= [D^1(t, \mathbf{x}(t)) \ D^2(t, \mathbf{x}(t)) \ D^3(t, \mathbf{x}(t)) \ D^4(t, \mathbf{x}(t))] \end{aligned} \quad (1.2)$$

are vectors describing the compartments which comprise the population:

- the population that is **susceptible (S)** to the disease,
- the population that has been **exposed (E)** to the disease and is not yet infectious,
- the population that is **infectious (I)** with a possible ailing outcome,
- the population that has **recovered (R)** from the disease,
- the population that is **vaccinated (V<sub>-</sub>)** but is not yet protected,
- the population that is **vaccinated (V<sub>+</sub>)** and is protected, and
- the population which is **deceased (D)**,

for each age group. These age groups are indicated by the superscripts 1, 2, 3, 4 corresponding to the age groups 0 – 17, 18 – 39, 40 – 64, and 65+ respectively. Moreover, superscript  $l$  indicates the vaccines that are deployed in the population.

Moreover, the system functions

$$\mathbf{f}_k(t, \mathbf{x}(t)) = \begin{bmatrix} f_k^1(t, \mathbf{x}(t)) \\ f_k^2(t, \mathbf{x}(t)) \\ f_k^3(t, \mathbf{x}(t)) \\ f_k^4(t, \mathbf{x}(t)) \end{bmatrix}, \quad (1.3)$$

where  $k \in \{S, E, I, R, V_+^l, V_-^l, D\}$ , are defined and for each age group  $i \in \{1, 2, 3, 4\}$  we define:

$$\dot{S}^i(t, \mathbf{x}(t)) = f_S^i(t, \mathbf{x}(t)) = -\lambda^i(t, \mathbf{I}(t)) \frac{S^i(t)}{N_i} + \xi_i R^i(t) + \psi_i V_+^{l,i}(t) \quad (1.4a)$$

$$\dot{E}^i(t, \mathbf{x}(t)) = f_E^i(t, \mathbf{x}(t)) = \lambda^i(t, \mathbf{I}(t)) \frac{S_{\text{total}}^i(t)}{N_i} - \sigma_i E^i(t) \quad (1.4b)$$

$$\dot{I}^i(t, \mathbf{x}(t)) = f_I^i(t, \mathbf{x}(t)) = \sigma_i E^i(t) - \gamma_i(t) I^i(t) - \eta_i(t) I^i(t) \quad (1.4c)$$

$$\dot{R}^i(t, \mathbf{x}(t)) = f_R^i(t, \mathbf{x}(t)) = \gamma_i(t) I^i(t) - \xi_i R^i(t) \quad (1.4d)$$

$$\dot{V}_-^{l,i}(t, \mathbf{x}(t)) = f_{V_-}^{l,i}(t, \mathbf{x}(t)) = -\lambda^i(t, \mathbf{I}(t)) \frac{V_-^{l,i}(t)}{N_i} - \rho_l \frac{w_b^{i,l}}{\tau_l} V_-^{l,i}(t) \quad (1.4e)$$

$$\dot{V}_+^{l,i}(t, \mathbf{x}(t)) = f_{V_+}^{l,i}(t, \mathbf{x}(t)) = \rho_l \frac{w_b^{i,l}}{\tau_l} V_-^{l,i}(t) - \psi_i V_+^{l,i}(t) \quad (1.4f)$$

$$\dot{D}^i(t, \mathbf{x}(t)) = f_D^i(t, \mathbf{x}(t)) = \eta_i(t) I^i(t) \quad (1.4g)$$

where

$$\lambda^i(t, \mathbf{I}(t)) = \sum_{j \in \{1,2,3,4\}} a_{j,i}(t)[1 - v_{j,i}(t)]I^j(t), \quad (1.5)$$

$$V_-^i(t) = \sum_{l \in \{1, \dots, k_v\}} V_-^{l,i}(t), \quad V_+^i(t) = \sum_{l \in \{1, \dots, k_v\}} V_+^{l,i}(t), \quad (1.6)$$

$$S_{\text{total}}^i(t) = S^i(t) + V_-^i(t) \quad (1.7)$$

$N_i$  denotes the number of individuals at age-group  $i$  and is defined as

$$N_i = S^i(t) + E^i(t) + I^i(t) + R^i(t) + V_+^i(t) + V_-^i(t) + D^i(t) \quad (1.8)$$

for all  $t \geq 0$ , since neither vital dynamics nor aging are considered in this model. For the total population  $N$ , it is

$$N = \sum_{i=1}^4 N_i \quad (1.9)$$

Throughout this work, only the dependency of the system states (defined in Paragraphs 1.2.1 and 1.2.2) from variable  $t$  is denoted for simplicity. The dependency from the state and input vectors will be denoted whenever it needs to be emphasized.

## Description of the Modelled Characteristics of COVID-19

COVID-19 disease is observed to affect people regardless of age differently, with older individuals exhibiting higher mortality rates [14, 32, 33] and longer recovery time [34]. Moreover, the incubation period of COVID-19 is higher for older individuals (aged 65 or older) [35, 36] and transmissibility begins 1-3 days prior to symptom onset [37]. Research suggests that immunity that is acquired by exposure to the SARS-CoV-2 virus is temporary [38, 39] as seroprevalence among individuals drops depending on the age of the individual [40]. Parameters  $a_{j,i}(t)$  and  $\eta_i(t)$  are generally chosen to be time-varying. A variety of factors may influence the values of these parameters. For example,  $a_{j,i}(t)$  is expected to drop during the warm seasons as people tend to move outdoors and/or indoor spaces are better ventilated. Viral transmutations can also cause variability in these parameters. Furthermore, there may be a relation among the NPI measures and the fatality rates, as investigated in Section 4.

Age-varying system parameters are indicated by their corresponding subscripts and are presented in Table 1.2.

Parameter	Description
$a_{j,i}(t)$	number of effective contacts among infectious individuals at age-group $j$ and susceptible people at age-group $i$
$\sigma_i$	rate in which an infected person becomes infectious
$\gamma_i$	recovery rate for an infected individual
$\eta_i(t)$	fatality rate of an infected individual
$\xi_i$	rate of loss of naturally acquired immunity at age group $i$
$\psi_i$	rate of loss of vaccination-induced immunity at age group $i$
$v_{j,i}(t)$	non-pharmaceutical interventions among susceptibles at age group $i$ and infectious at age group $j$
$w_b^{l,i}$	efficacy rate of vaccine $l$ for age-group $i$ at second dose
$\rho_l$	rate of attendance for 2nd dose for vaccine $l$
$\tau_l$	time interval between 1st dose and immunization for vaccine $l$

**Table 1.2:** Brief overview of system parameters.

## 1.2.2 Proposed Model with Control

In addition to the disease dynamics described by (Eq. 1.4), we introduce the system with control input vector  $\mathbf{u}$ , defined as:

$$\mathbf{u}(t) = [\mathbf{u}_1(t) \quad \mathbf{u}_2(t) \quad \mathbf{u}_3(t) \quad \mathbf{u}_4(t)]^\top \in \mathbb{R}^m$$

where  $\mathbf{u}_i(t) = [u^{1,i} \quad \dots \quad u^{k_v,i}]$  describes the vaccination strategy employed upon age-group  $i$ .  $k_v$  denotes the total number of vaccines used.

By augmenting the initial system functions of (Syst. 1.4) with the control variables, we receive:

$$\dot{S}^i(t, \mathbf{x}(t), \mathbf{u}(t)) = f_S^i(t, \mathbf{x}(t), \mathbf{u}(t)) = f_S^i(t, \mathbf{x}(t)) - \sum_{l=1}^{k_v} u^{l,i}(t) \quad (1.10a)$$

$$\dot{E}^i(t, \mathbf{x}(t)) = f_E^i(t, \mathbf{x}(t)) = f_E^i(t, \mathbf{x}(t)) \quad (1.10b)$$

$$\dot{I}^i(t, \mathbf{x}(t)) = f_I^i(t, \mathbf{x}(t)) = f_I^i(t, \mathbf{x}(t)) \quad (1.10c)$$

$$\dot{R}^i(t, \mathbf{x}(t)) = f_R^i(t, \mathbf{x}(t)) = f_R^i(t, \mathbf{x}(t)) \quad (1.10d)$$

$$\dot{V}_-^{l,i}(t, \mathbf{x}(t), \mathbf{u}(t)) = f_V^{l,i}(\mathbf{x}(t), \mathbf{u}(t)) = f_V^{l,i}(\mathbf{x}(t)) + u^{l,i}(t) \quad (1.10e)$$

$$\dot{V}_+^{l,i}(t, \mathbf{x}(t)) = f_{V_+}^{l,i}(\mathbf{x}(t)) = f_{V_+}^{l,i}(\mathbf{x}(t)) \quad (1.10f)$$

$$\dot{D}^i(t, \mathbf{x}(t)) = f_D^i(t, \mathbf{x}(t)) = f_D^i(t, \mathbf{x}(t)) \quad (1.10g)$$

It is now evident that the model with control Eq. (1.10) is in the **affine in the**

**control** form, which can prove useful when applying Pontryagin's Principle:

$$\dot{\mathbf{x}}(t, \mathbf{x}(t), \mathbf{u}(t)) = \mathbf{f}(t, \mathbf{x}(t)) + \mathbf{B}\mathbf{u}(t) \quad (1.11)$$

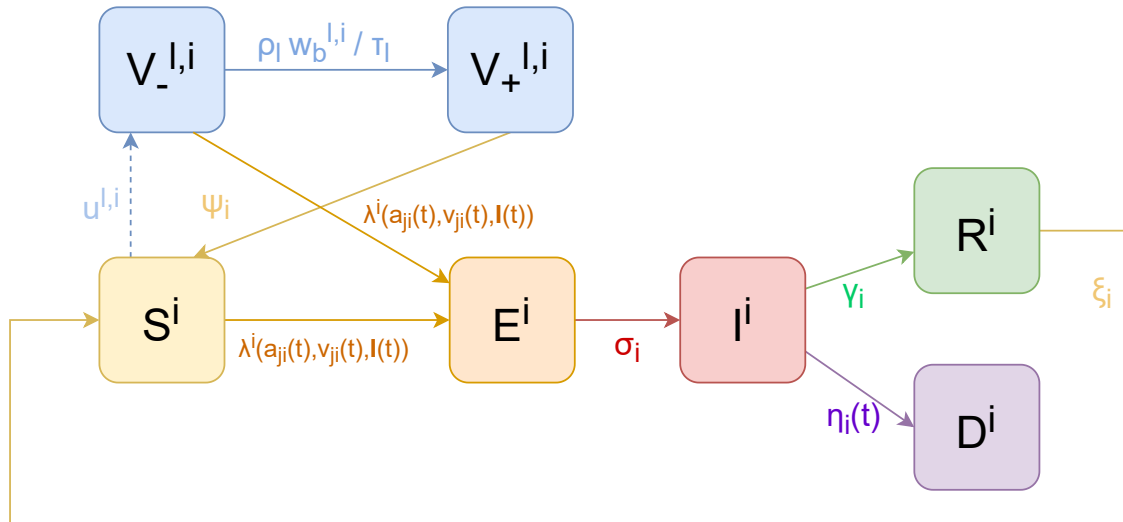


**Figure 1.1:** Schematic representation of the compartment transitions for the proposed model with control.

# Chapter 2

## System Output and Measurements

### 2.1 Introduction

This chapter focuses on defining the system outputs and presenting the methodology for collecting the data (measurements) that can describe the system outputs. The system states cannot always be directly inferred; for example, it is not possible to keep measurements of the number of infected individuals who are exposed in each age group (system states  $E^i(t)$ ) and do not transmit the disease. However, based on the data of the total number of cases for each age group, these states can be made observable in the output of system.

Of course, the preceding discussion makes clear that there is a close relation between the system outputs and the measurements. The system outputs, given as a linear combination of the system states, should be defined so as to match the available measurements.

For the system with control defined in Paragraph 1.2.2, the system outputs  $\mathbf{y} \in \mathbb{R}^{n_y}$  are defined in the following manner:

$$\begin{aligned}\dot{\mathbf{x}}(t) &= \mathbf{f}(\mathbf{x}(t)) + \mathbf{B}\mathbf{u}(t) \\ \mathbf{y}(t) &= \mathbf{C}\mathbf{x}(t)\end{aligned}\tag{2.1}$$

In Section 2.2, the available data from the disease spreading in Greece are assessed and in Section 2.4.1, the system outputs are defined so as to match the data.

## 2.2 Collection of Data

In this study, national data from Greece are collected, processed and utilized as a study case. The collection of data satisfies the following criteria:

- the collected data must adequately contain information corresponding to our model's characteristics as much as possible, for example data per age-group, and
- the collected data must originate from reliable sources

Taking all of the above into consideration, the measurement data originate from the publicly available data from the Greek National Public Health Organization (EODY) [41], the Johns Hopkins University [42] [43] and the Hellenic Government [44]. The following measurements were collected from these sources:

- daily confirmed cases per age-group and as a total since the beginning of the pandemic [41, 45],
- daily registered deaths per age-group and as a total over the same period [41, 45],
- cumulative recovered cases of the population as a total [43],
- cumulative vaccinations as a total for all age groups [44].

## 2.3 System Outputs

In this section the system outputs described in (2.1) are formulated. Given the available data mentioned in Section 2.2, it is now evident that from the system with controls the following outputs should be provided:

- the cumulative daily cases for each age group,  $y_{\text{cases}}^i(t)$
- the cumulative daily deaths for each age group,  $y_{\text{deaths}}^i(t)$
- the cumulative daily number of vaccinated individuals for each age group,  $y_{\text{vaccinated}}^i(t)$
- the number of recovered cases,  $y_{\text{recovered}}(t)$

The cumulative cases per age group  $i$  at a day  $t$  consist of all cases of group  $i$  up to day  $t$ . Each of these cases can be found either in states  $E^i(t)$ ,  $I^i(t)$ ,  $R^i(t)$  or  $D^i(t)$ , or in the  $S^i(t)$  compartment since immunity is impermanent. Define the vector for total cumulative cases  $\mathbf{y}_{\text{cases}}(t)$ :

$$\mathbf{y}_{\text{cases}}(t) := \begin{bmatrix} y_{\text{cases}}^1(t) \\ y_{\text{cases}}^2(t) \\ y_{\text{cases}}^3(t) \\ y_{\text{cases}}^4(t) \end{bmatrix} = \begin{bmatrix} E^1(t) + I^1(t) + R^1(t) + D^1(t) \\ E^2(t) + I^2(t) + R^2(t) + D^2(t) \\ E^3(t) + I^3(t) + R^3(t) + D^3(t) \\ E^4(t) + I^4(t) + R^4(t) + D^4(t) \end{bmatrix} \quad (2.2)$$

Due to the definition of the state equations in Sections 1.2.1 and 1.2.2, the number of individuals that have lost naturally acquired immunity over time cannot be deduced using a linear combination of the system states. This introduces a *systematic error* between the system outputs and the measurements.

Similarly, the deaths per age group  $i$  are found in state  $D^i(t)$ . Define the vector for total cumulative deaths  $\mathbf{y}_{\text{deaths}}(t)$ :

$$\mathbf{y}_{\text{deaths}}(t) := \begin{bmatrix} y_{\text{deaths}}^1(t) \\ y_{\text{deaths}}^2(t) \\ y_{\text{deaths}}^3(t) \\ y_{\text{deaths}}^4(t) \end{bmatrix} = \begin{bmatrix} D^1(t) \\ D^2(t) \\ D^3(t) \\ D^4(t) \end{bmatrix} \quad (2.3)$$

The total number of vaccinated individuals at age group  $i$  using vaccine  $l$ ,  $y_{\text{vaccinated}}^{l,i}(t)$ , are found in states  $V_-^{l,i}(t)$  or  $V_+^{l,i}(t)$ . Define the vector for the number of vaccinated individuals  $\mathbf{y}_{\text{vaccinated}}(t)$ :

$$\mathbf{y}_{\text{vaccinated}}(t) := \begin{bmatrix} y_{\text{vaccinated}}^{1,1}(t) \\ y_{\text{vaccinated}}^{2,1}(t) \\ \dots \\ y_{\text{vaccinated}}^{k_n,1}(t) \\ \dots \\ y_{\text{vaccinated}}^{1,4}(t) \\ y_{\text{vaccinated}}^{2,4}(t) \\ \dots \\ y_{\text{vaccinated}}^{k_n,4}(t) \end{bmatrix} = \begin{bmatrix} V_-^{1,1}(t) + V_+^{1,1}(t) \\ V_-^{2,1}(t) + V_+^{2,1}(t) \\ \dots \\ V_-^{k_n,1}(t) + V_+^{k_n,1}(t) \\ \dots \\ V_-^{1,4}(t) + V_+^{1,4}(t) \\ V_-^{2,4}(t) + V_+^{2,4}(t) \\ \dots \\ V_-^{k_n,4}(t) + V_+^{k_n,4}(t) \end{bmatrix} \quad (2.4)$$

The number of recovered individuals for all age groups is given by:

$$y_{\text{recovered}}(t) := \sum_{i=1}^4 R^i(t) \quad (2.5)$$

The system output vector  $\mathbf{y}(t)$  becomes:

$$\mathbf{y}(t) = \begin{bmatrix} \mathbf{y}_{\text{cases}}(t) \\ \mathbf{y}_{\text{deaths}}(t) \\ y_{\text{recovered}}(t) \\ \mathbf{y}_{\text{vaccinated}}(t) \end{bmatrix} \quad (2.6)$$

Observing the number of the recovered individuals,  $y_{\text{recovered}}(t)$ , as well as the number of deaths for each group  $y_{\text{deaths}}(t)$  and the number of vaccinated individuals ( $y_{\text{vaccinated}}^i(t)$ ) is specifically important for the control strategy in order to minimize death counts and achieve herd immunity.

## 2.4 Data Processing

The collected data for the confirmed cases can only describe the detected cases of COVID-19. Misreporting of the COVID-19 cases can lead to a false epidemiological profile of the disease in the population. Therefore we need to make a prediction of the true number of cases by estimating the IFR of COVID-19.

The system outputs  $y_{\text{vaccinated}}^i(t)$  describe the individuals who have received the first dose from the vaccine. These individuals reside in the state  $V_-^{i,l}(t)$  for a mean time equivalent to the time period between the two doses and the time required to acquire immunity before transitioning to state  $V_+^{l,i}(t)$ . Moreover, the available data on the vaccinations do not pertain to each age group, but rather as a total for all age groups.

In this section, the estimation methodology for the true number of COVID-19 cases is proposed and the methodology used to process the data available on vaccinations is presented.

### 2.4.1 Estimation of the True Number of COVID-19 Cases

As COVID-19 disease can spread asymptotically in the population, discrepancy between the true number of cases and the reported number of cases can be expected. Therefore, the reported number of cases may not be able to capture the true extend of the pandemic. In order to infer an estimation for the true cases, we turn our focus on the reported number of deaths, as these measurements are considered accurate.

The IFR (Infection Fatality Rate) is a key parameter for the estimation of the true scale of COVID-19. This parameter expresses the ratio of deaths due to COVID-19 to the true number of COVID-19 infections and is different from CFR (Case Fatality Rate), which is simply the ratio of COVID-19 deaths to reported number of COVID-19 infections. As the IFR cannot be fully determined amidst the pandemic, it has to be estimated.

As IFR is typically lower than the CFR, the IFR can be estimated by the lowest CFR among different countries. Two countries with consistently low reported CFR are Germany and South Korea. [46, 47] We choose Germany as the benchmark country in order to estimate IFR, as the disease dynamics may be more cohesive between Greece and Germany (for example, because of the circulation of viral mutations throughout Europe, etc.).

The estimated true number of cases is given by:

$$C_{\text{est.}}^i(t) = \frac{D^i(t + \tau_d)}{\text{IFR}_{\text{est.}}^i} \quad (2.7)$$

where  $\tau_d$  indicates the delay from exposure to death.

Due to the low fatality in the age group 1, however, we may not be able to infer a prediction for this age group. Research suggests that most COVID-19 infections originate from the 2nd and 3rd age groups [48] and that individuals in age group 1 are overall less susceptible to the disease [49]. Therefore, we do not propose a prediction for age group 1.

The prediction for the true number of cases is used from the 4th week since the beginning of the pandemic. The data for reported cases (eg. the data for the 1st age group) have been shifted to account for the delay from exposure to reporting ( $\tau_r$ ).

## 2.4.2 Processing of the Vaccination Data

Since the data for vaccinations for each age group and for each vaccine is not available, we must also estimate the number of vaccinations for each group.

As of early-April 2021[50]:

- 67% of vaccinations were done using the BNT162b2 vaccine,
- 25% of vaccinations were done using the AZD1222 vaccine, and
- 8% of vaccinations were done using mRNA-1273 vaccine.

Up to that time, the vaccination of healthcare professionals (H.P.) was initiated. The number of healthcare professionals in 2020 is estimated to be approx. 95,000 [51]. No further information has been presented regarding the percentage of healthcare professionals having been vaccinated as of April 2021 and their age distribution. We assume that 70% of H.P. have been vaccinated and that they are evenly distributed in age-groups 2 and 3.

# Chapter 3

## Parameter Specification

### 3.1 Introduction

In order for the model to describe the dynamics of the disease in Greece, the parameters of the system must be suitably chosen. The model's parameters will be specified from system identification, bibliography and by manual selection.

Some of the system parameters' values can be inferred from the bibliography, given that these parameters have been sufficiently studied in the bibliography. Parameters whose values are not known in advance are found using system identification techniques. Since the solution of the minimization problem of the functional, defined in Section 3.2.2, is not unique, the a-priori knowledge of the values of some parameters (e.g., from the bibliography) can help lead the minimization problem to converge to the solution closer to the actual one.

Table 3.1 presents the methods used to define the system parameters. In the following section, the system identification problem is presented and formulated.

### 3.2 System Identification

In order to identify the system's parameters, functions `idnlgrey` and `nlgreyest` from MATLAB's System Identification Toolbox. A brief overview of these functions is given below:

`idnlgrey`: this function serves as a wrapper for the non-linear grey-box model for

Parameter	Specification Method
$a_{j,i}(t)$	system identification
$\sigma_i$	bibliography
$\gamma_i$	system identification
$\eta_i(t)$	system identification / manual fitting
$\xi_i$	bibliography
$v_{j,i}(t)$	system identification / manual fitting
$u_{j,i}(t)$	system identification
$w_b^{l,i}$	bibliography
$\rho_l$	bibliography
$\tau_l$	bibliography

**Table 3.1:** Brief overview of the methods used to specify the parameter values.

use in `nlgreyest`. The system functions (written in an `.m` file), along with the system's initial conditions and the initial parameter values, are given as input in the function.

`nlgreyest`: this function performs the system identification. It receives the identification data, the model specification from `idnlgrey` and optionally an object of class `nlgreyestOptions` as function inputs. `nlgreyestOptions` allows us to declare the specifications for the parameter estimation.

## Data Specification for System Identification

In order for the system to be identified, the system outputs must be related to the data. Based on the preceding discussion in Chapter 2, one can infer the following relation between the measurements for the cumulative cases for the age group  $i$ ,  $\text{cases}^i(t)$ , and the system outputs:

$$\text{cases}^i(t) \equiv y_{\text{cases}}^i(t) \quad (3.1)$$

Similarly, the measurements for the number of recovered individuals  $\text{recovered}^i(t)$  are related to the system outputs in this way:

$$\text{recovered}(t) \equiv y_{\text{recovered}}(t) \quad (3.2)$$

and the relation between the measurements for vaccinations performed in age group  $i$  with the vaccine  $l$  defined as  $\text{vaccinated}^{l,i}(t)$  and the system outputs is given by:

$$\text{vaccinated}^{l,i}(t) \equiv y_{\text{vaccinated}}^{l,i}(t) \quad (3.3)$$

Last, the relation between the cumulative deaths for the age-group  $i$ , defined as  $\text{deaths}^i(t)$  and the system outputs are given by:

$$\text{deaths}^i(t) \equiv y_{\text{deaths}}^i(t) \quad (3.4)$$

Data since the outbreak of the epidemic up to mid August 2020 was used for the system identification of the parameter values during 1st wave. In order to identify the system properly, it is important to provide initial parameter values based on a-priori knowledge wherever applicable. Having identified the system parameters for the 1st wave, providing suitable initial parameters for the 2nd wave is possible. The problem of identifying the system parameters pertains to Grey-Box System Modelling, since the functions of the system dynamics are determined in advance.

### 3.2.1 Defining the Initial System States

As the delays from exposure to reporting and from exposure to death have been accounted for in the data, the system initial system states are given by:

$$\mathbf{x}_0 = [\mathbf{S}_0 \ \mathbf{E}_0 \ \mathbf{I}_0 \ \mathbf{R}_0 \ \mathbf{V}_{-0}^l \ \mathbf{V}_{+0}^l \ \mathbf{D}_0]^\top$$

where

$$\begin{aligned} \mathbf{S}_0 &= [N(1) \ N(2) - 1 \ N(3) \ N(4)], \\ \mathbf{E}_0 &= [0 \ 1 \ 0 \ 0], \\ \mathbf{I}_0 &= [0 \ 0 \ 0 \ 0], \\ \mathbf{R}_0 &= [0 \ 0 \ 0 \ 0], \\ \mathbf{V}_{-0}^l &= [0 \ 0 \ 0 \ 0], \\ \mathbf{V}_{+0}^l &= [0 \ 0 \ 0 \ 0], \\ \mathbf{D}_0 &= [0 \ 0 \ 0 \ 0] \end{aligned} \quad (3.5)$$

### 3.2.2 Estimating the System Parameters

System identification involves the minimization of the cost function

$$C(\mathbf{p}) = \sum_{t=1}^N \mathbf{e}^\top(t, \mathbf{p}) \mathbf{W} \mathbf{e}(t, \mathbf{p}) + \frac{1}{N} \lambda (\mathbf{p} - \mathbf{p}^*)^\top \mathbf{R} (\mathbf{p} - \mathbf{p}^*) \quad (3.6)$$

where  $\mathbf{e}(t, \mathbf{p}) \in \mathbb{R}^{n_y}$  is a vector containing the error between estimated output and measured data for some  $t \leq N$ ,  $t \in \mathbb{N}$ ,  $\mathbf{W} \in \mathbb{R}^{n_y \times n_y}$  is a positive semi-definite matrix

containing the weights corresponding to each output for identification,  $\mathbf{p} \in \mathbb{R}^{n_p}$  and  $\mathbf{p}^* \in \mathbb{R}^{n_p}$  are vectors containing the estimated values of the system parameters at each iteration of the cost function optimization and the initial parameter values, respectively.  $\lambda$  and  $\mathbf{R}$  are referred to as the regularization value and weighting vector, respectively. The second term is referred to as the regularization term of the minimization problem and will be explained later in this section.

The output weighting matrix  $\mathbf{W}$  allows us to define the *relative importance* of each output to be identified. Throughout the scope of this work,  $\mathbf{W}$  will be considered as a diagonal matrix, with each of the diagonal elements  $w_{i,j}$ ,  $i = j$ , corresponding to the weighting factor of each output. Thus, the first term of the cost function becomes a weighted sum of the squared errors of the outputs  $e_i(t, \mathbf{p})$  for all  $t \leq N$ . The second term also becomes a weighted sum of the square error between the estimated parameter values and their initial values:

$$C(\mathbf{p}) = \sum_{t=1}^N \sum_{i=1}^{n_y} w_{i,i} e_i^2(t, \mathbf{p}) + \frac{\lambda}{N} \sum_{i=1}^{n_p} r_i (p_i - p_i^*)^2 \quad (3.7)$$

It was observed that identifying the system using the identity matrix as  $\mathbf{W}$  results in poor fitting for the outputs related to the deceased individuals  $y_{\text{deaths}}^i(t)$ . By trial and error, it is found that the selection of much larger weights for these compartments resulted in better fitting for the deceased compartments. This, however, comes with the price of less accurate fitting of the outputs related to the total *cases*.

**Regularization** allows us to overcome this limitation by inserting a term in the cost function which penalizes large deviations of some of the estimated parameters from their initial values. This is of significant importance as we can allow the system identification to focus on the outputs for the *total cases* and the *recovered* cases as long as we can provide relatively accurate initial values for  $\eta_i$ .  $\mathbf{R}$  is a vector of non-negative elements for defining the regularization weights for each parameter and  $\lambda > 0$  is a constant value for determining the penalty the deviation from the initial parameter values, often referred to as the *bias versus variance tradeoff*.

As the data for the recovered cases originate from a model prediction, we choose low weight value for identifying the recovered individuals. Moreover, the values for  $\gamma_i$  were constrained to a maximum value according to [52] and larger initial values were assigned to the younger age groups. A small regularization weight on  $\gamma_i$  was also applied in order to prevent them from getting unreasonably large deviations from the initial estimations.

# Chapter 4

## Results And Discussion

### 4.1 Estimation of the True Number of COVID-19 Cases

Using  $\tau_d = 18$  days [53] and  $\tau_r = 6$  days [36], we obtain the estimation presented in Fig. 4.1 in comparison to other prediction models such as the ICL and IHME model [54, 55].

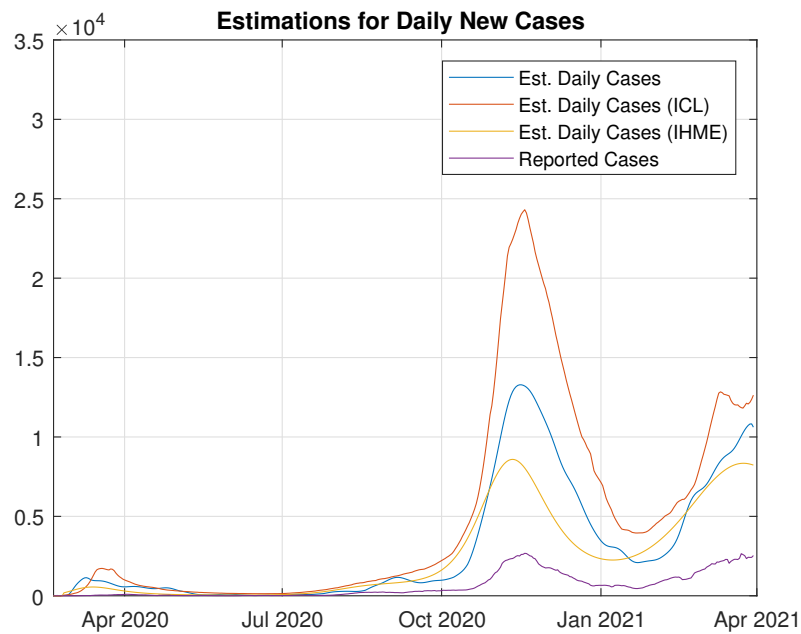


**Figure 4.1:** Estimated daily incidence data.

As can be noticed from Fig. 4.1, large deviations can occur among different approaches to estimating the true number of infections. A major factor that causes this deviation is the different estimation of the IFR parameter among these models. For example, the ICL model uses estimations of IFR from data in China [56]. The estimation of true infections projected in this work falls between the estimations of these models.

### 4.1.1 Basic Reproduction Number ( $R_0$ ) and $R_t$

One substantial parameter characteristic of a pandemic is the basic reproduction number  $R_0$ . Using the EpiEstim package in R, we examine the evolution of  $R_t$  and obtain  $R_0$  in the beginning of the pandemic. Assuming a serial interval with mean  $\mu = 5.2$  days [ 95% C.I.: (3.6 days, 6.8 days) ] [57], we compute the  $R_t$  on a 10-day sliding window.

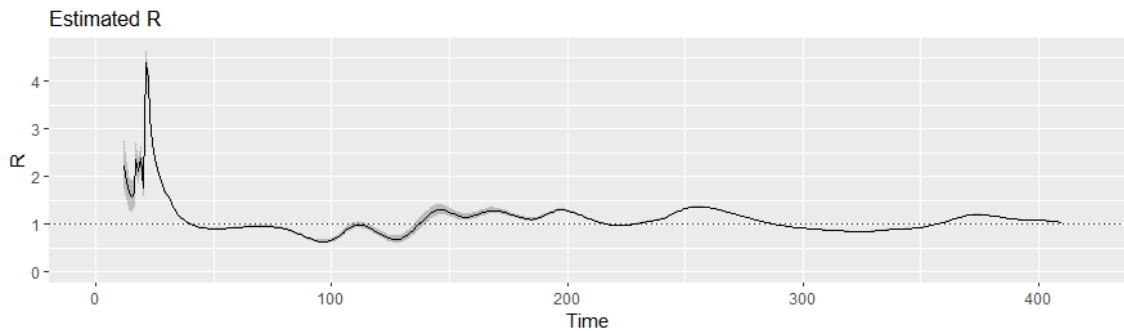


**Figure 4.2:** Evolution of  $R_t$  computed on a 10-day sliding window.

The results are presented in Fig. 4.2.  $R_t$  exhibits a spike early in the pandemic, which can be attributed to the estimation of the true number of cases that we adopted after the 21st day since the beginning of the pandemic. It can be seen that  $R_t$  remains slightly above 1.00 in mid-April 2021. The estimated  $R_t$  was announced by governmental authorities to be 1.02, presenting a small drop since March of 2021 [58]. Furthermore,  $R_0$  is estimated to be 2.217.  $R_0$  in Greece was estimated to be slightly below 2.50 [52].

## 4.2 Parameter Specification

The final parameter values are presented in Table 4.1 and Table 4.2. Table 3.1 presents the methods used for specifying each parameter.

Parameter	Value	Parameter	Value	Parameter	Value
$a_{1,1}(t)$	Fig. 4.4	$\eta_1(t)$	Fig. 4.5	$v_{j,1}(t)$	Fig. 4.3
$a_{2,1}(t)$	Fig. 4.4	$\eta_2(t)$	Fig. 4.5	$v_{j,2}(t)$	Fig. 4.3
$a_{3,1}(t)$	Fig. 4.4	$\eta_3(t)$	Fig. 4.5	$v_{j,3}(t)$	Fig. 4.3
$a_{4,1}(t)$	Fig. 4.4	$\eta_4(t)$	Fig. 4.5	$v_{j,4}(t)$	Fig. 4.3
$a_{1,2}(t)$	Fig. 4.4	$\gamma_1$	0.0879	$w_b^{i,l}$	Table 4.2
$a_{2,2}(t)$	Fig. 4.4	$\gamma_2$	0.1024	$\tau_l$	Table 4.2
$a_{3,2}(t)$	Fig. 4.4	$\gamma_3$	0.0976	$\rho_l$	Table 4.2
$a_{4,2}(t)$	Fig. 4.4	$\gamma_4$	0.0507		
$a_{1,3}(t)$	Fig. 4.4	$\xi_1, \psi_1$	0.0056		
$a_{2,3}(t)$	Fig. 4.4	$\xi_2, \psi_2$	0.0056		
$a_{3,3}(t)$	Fig. 4.4	$\xi_3, \psi_3$	0.0056		
$a_{4,3}(t)$	Fig. 4.4	$\xi_4, \psi_4$	0.0056		
$a_{1,4}(t)$	Fig. 4.4	$\sigma_1$	0.1670		
$a_{2,4}(t)$	Fig. 4.4	$\sigma_2$	0.1670		
$a_{3,4}(t)$	Fig. 4.4	$\sigma_3$	0.1670		
$a_{4,4}(t)$	Fig. 4.4	$\sigma_4$	0.1000		

**Table 4.1:** Final system parameter values.

The values for  $\xi_i$  were chosen in accordance with [39]. The  $\sigma_i$  values were chosen according to [35, 37]. The efficacy rates of the vaccination varies depending on the vaccine used [54].

### 4.2.1 Vaccination Parameters

As of April 2021, three vaccines have been approved for administration to the general population: *BNT162b2* (Pfizer-BioNTech), *AZD1222* (AstraZeneca) and *mRNA-1273* (Moderna).

The efficacy rates for the *BNT162b2* were obtained from [59, 60]. The efficacy rates for the *AZD1222* were obtained from [61].

Lastly, the probabilities of attendance for the second dose of the vaccine for each vaccine are approximated from the probability of attendance to the vaccination appointment for each vaccine obtained from [50].

Parameter	BNT162b2 Vaccine ( $l = 1$ )			
	Age Group 1	Age Group 2	Age Group 3	Age Group 4
$w_b^{1,i}$	0.950	0.950	0.950	0.950
$\tau_1$	21+15 d.	21+15 d.	21+15 d.	21+15 d.
$\rho_1$	0.970	0.970	0.970	0.970
Parameter	AZD1222 Vaccine ( $l = 2$ )			
	Age Group 1	Age Group 2	Age Group 3	Age Group 4
$w_b^{2,i}$	0.705	0.705	0.705	0.705
$\tau_2$	84+15 d.	84+15 d.	84+15 d.	84+15 d.
$\rho_2$	0.940	0.940	0.940	0.940
Parameter	mRNA-1273 Vaccine ( $l = 3$ )			
	Age Group 1	Age Group 2	Age Group 3	Age Group 4
$w_b^{3,i}$	0.940	0.940	0.940	0.864
$\tau_3$	28+15 d.	28+15 d.	28+15 d.	28+15 d.
$\rho_3$	0.970	0.970	0.970	0.970

**Table 4.2:** Final system parameter values for the vaccines.

## 4.2.2 Time-Varying System Parameters

### Non-Pharmaceutical Interventions $v_{j,i}(t)$

In order to simplify the complexity of the model, we consider that the Non-Pharmaceutical Interventions (NPIs) applied to a susceptible person at group  $i$  reduces the number of effective contact rates evenly for each age group  $j$  of the infected individuals ( $v_{1,i}(t) = \dots = v_{4,i}(t)$ ). During system identification, initial values for these parameters were chosen based on a qualitative timeline of the NPI in effect and a small regularization weight was applied. For the second wave onwards, these values were chosen manually in order to best fit the data.

As can be seen from the diagram, the effect of the NPI measurements typically follow the similar trends. Following the halt of the 1st lockdown order, a significant drop in  $u_{j,1}$  can be observed in the following weeks. Parameters  $u_{j,i}$ ,  $2 \leq i \leq 4$ , exhibit a drop at a latter time point. This can be attributed to the estimation of the true cases for age-groups 2, 3 and 4.

The values for the parameters  $v_{j,i}(t)$  are given in Fig. 4.3.

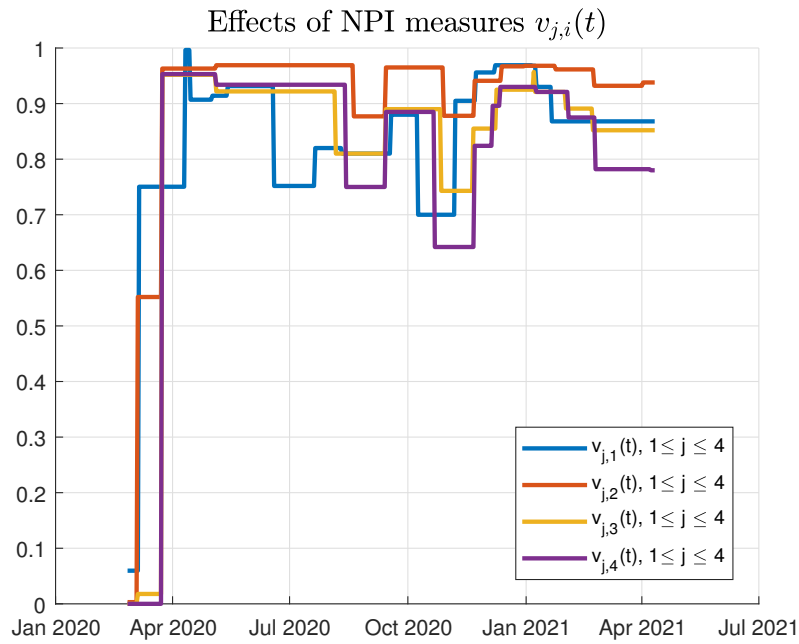


**Figure 4.3:** time-varying effects of NPI measures applied in population for each age group

### Number of Effective Contacts $a_{j,i}(t)$

During system identification, initial values for these parameters were chosen based on observation of the trend of the cases <sup>$i$</sup> ( $t$ ) measurements. On the second wave onwards, the values were chosen in such a way as to avoid large deviations of the parameters  $v_{j,i}(t)$  from the identified values on the first wave.

Indicative values for the parameters  $a_{j,i}(t)$  are given in Fig. 4.4. As can be seen, the numbers of effective contacts  $a_{j,i}(t)$  are higher from the second wave onwards. This rise can be attributed to the seasonal changes which might have led to indoor gatherings and the appearance of viral variants in early 2021.

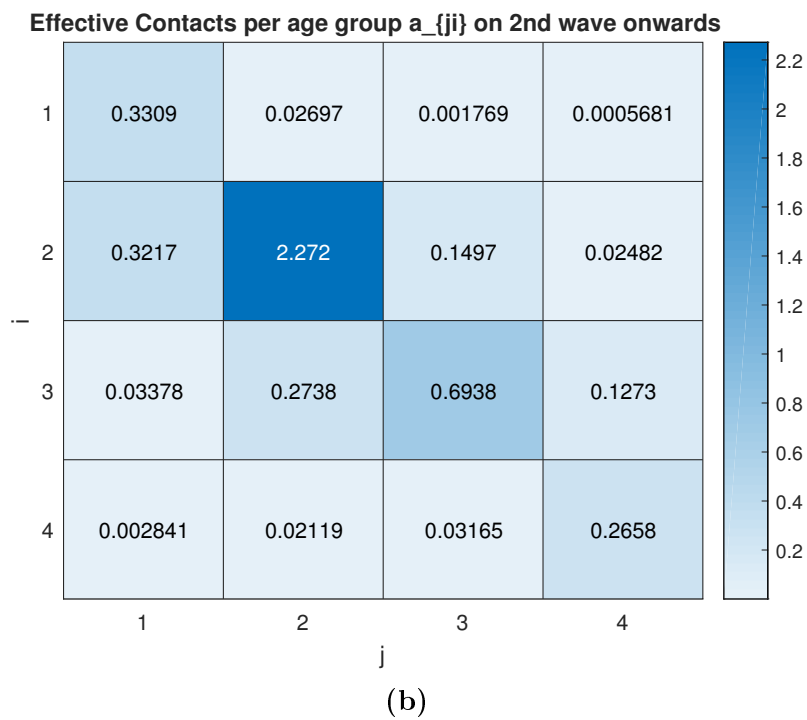
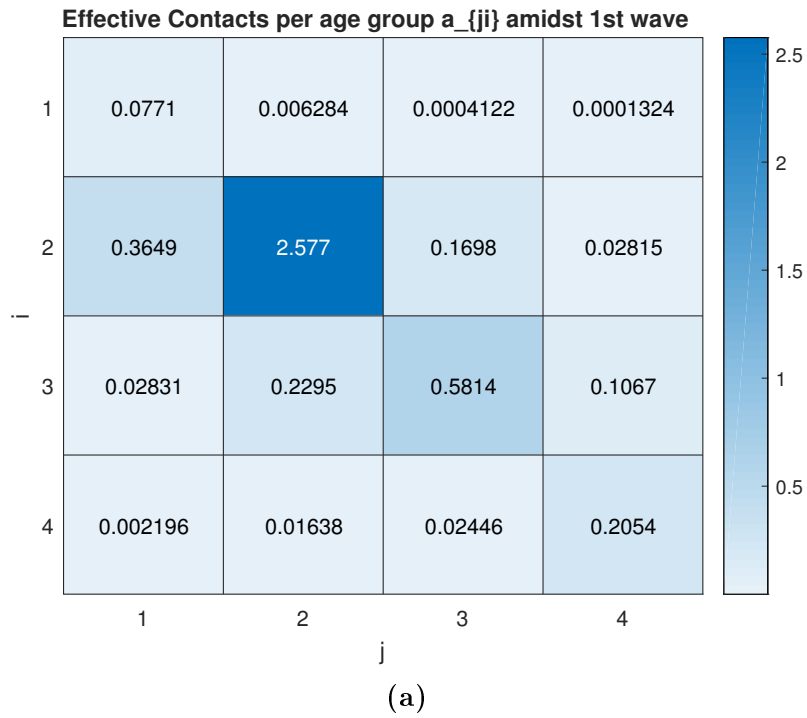
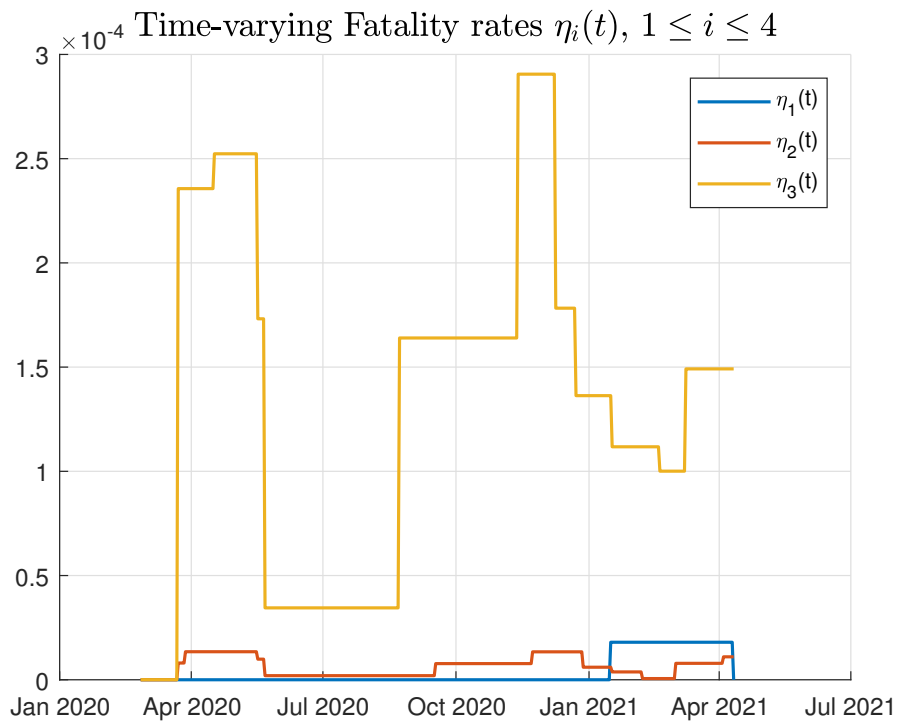


**Figure 4.4:** Effective contact rates for each pair  $(j,i)$  (a) during 1st wave (b) during 2nd wave onwards

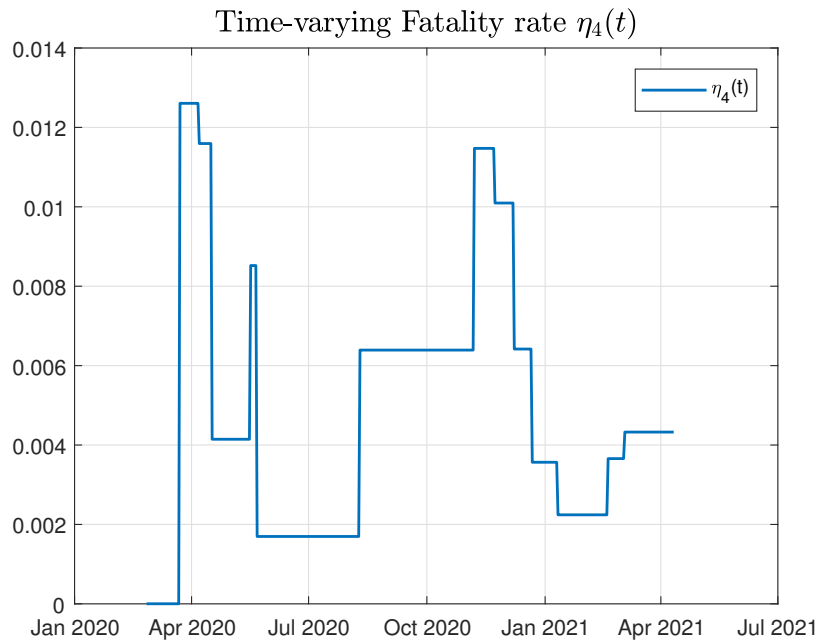
### Fatality Rates $\eta_i(t)$

Similarly, for the parameters  $\eta_i(t)$ , the values were identified during the first wave and were manually chosen to fit the day from the second wave onwards.

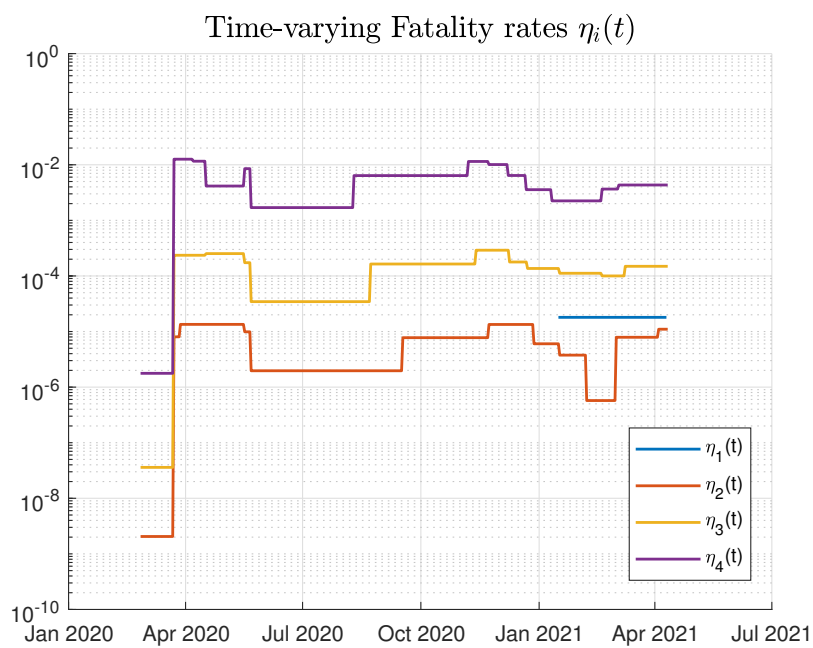
The values for the parameters  $\eta_i(t)$  are presented in Fig. 4.5. As can be seen, the fatality rates for  $i = 2, 3, 4$  tend to be almost equal at the peak of each wave. This might stand in contrast with the high rise of deaths observed in  $deaths^i(t)$  during the 2nd wave, however this can be attributed to the fact that the number of individuals in states  $I^i(t)$  might be higher from the second wave onwards in comparison to the first wave.



(a) Fatality rates  $\eta_i(t)$ ,  $1 \leq i \leq 3$  in linear scale



(b) Fatality rate  $\eta_4(t)$  in linear scale



(c) Fatality rates  $\eta_i(t)$  in logarithmic scale

**Figure 4.5:** Time-varying fatality rates for each age-group

### Control Inputs $u^{l,i}(t)$

The values for the control inputs  $u^{l,i}(t)$  until mid-April were chosen based on system identification.

The values for the parameters  $u^{l,i}(t)$  are presented in Fig. 4.6, Fig. 4.7 and Fig. 4.9. No vaccination has been performed on the youngest age group,  $i = 1$ .

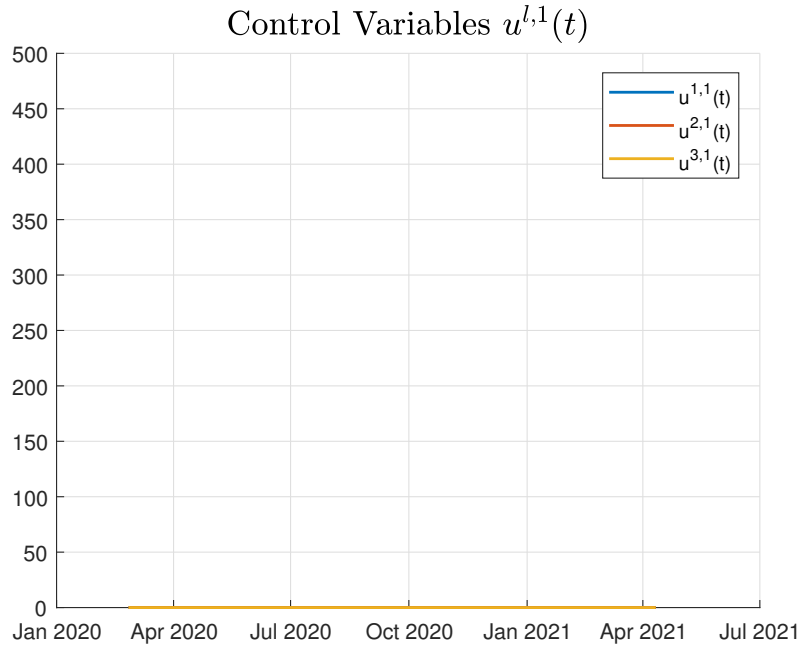


**Figure 4.6:** Values of control variables  $u^{l,1}(t)$

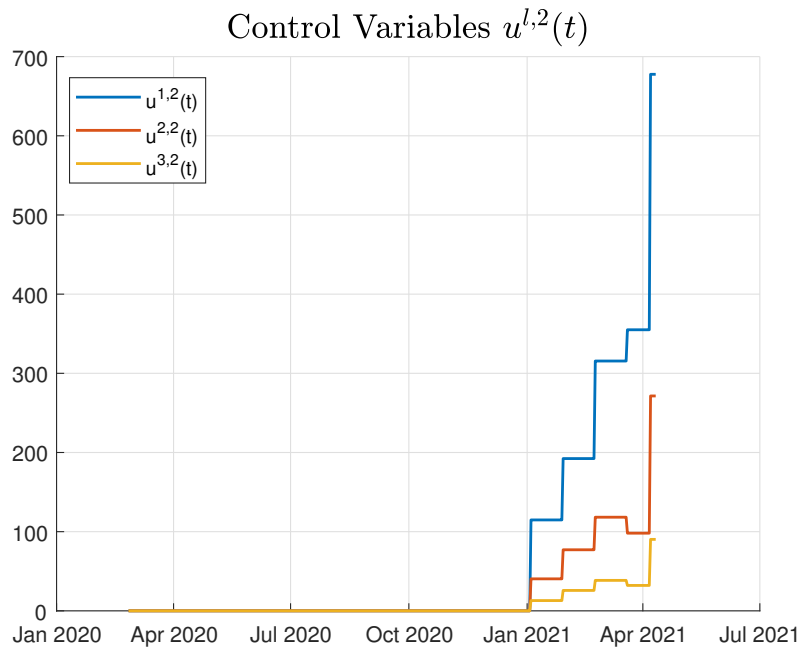


**Figure 4.7:** Values of control variables  $u^{l,2}(t)$

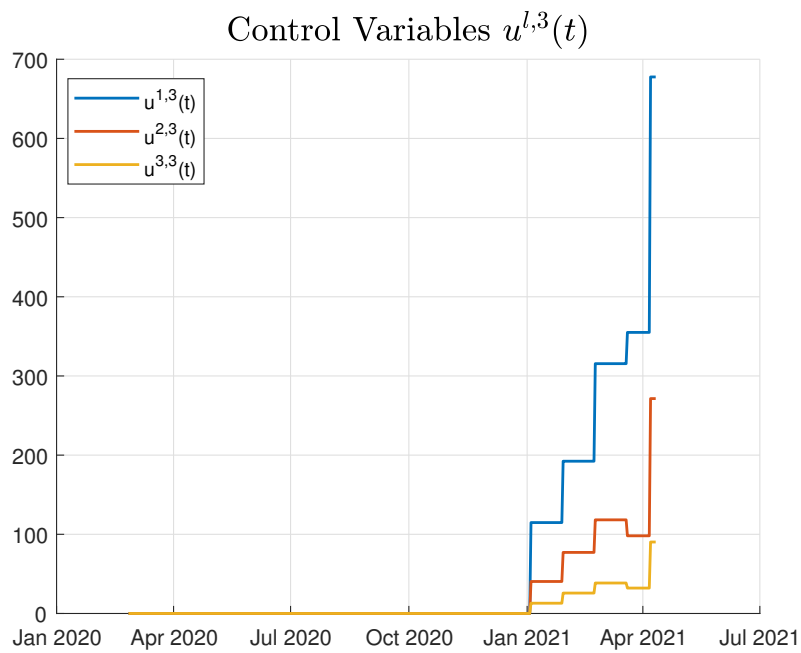


**Figure 4.8:** Values of control variables  $u^{l,3}(t)$

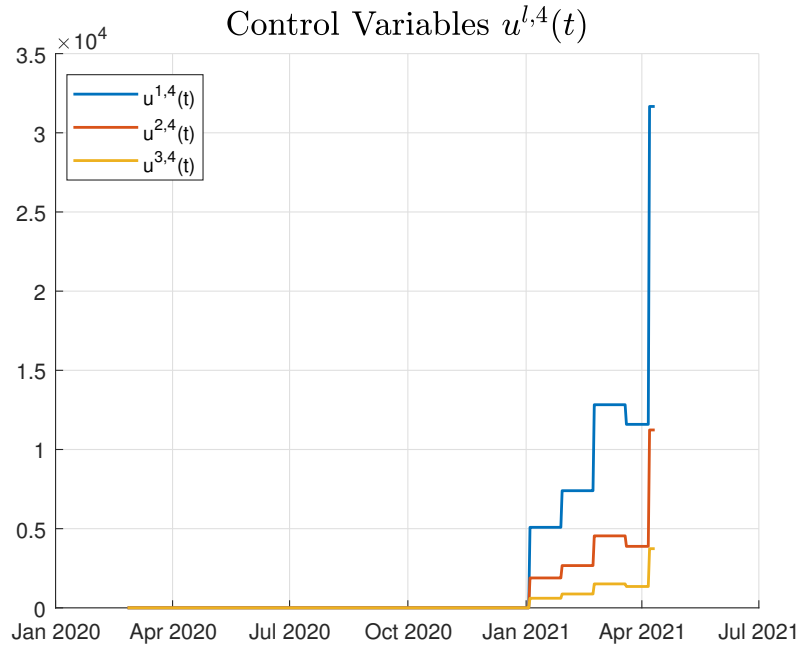


**Figure 4.9:** Values of control variables  $u^{l,4}(t)$

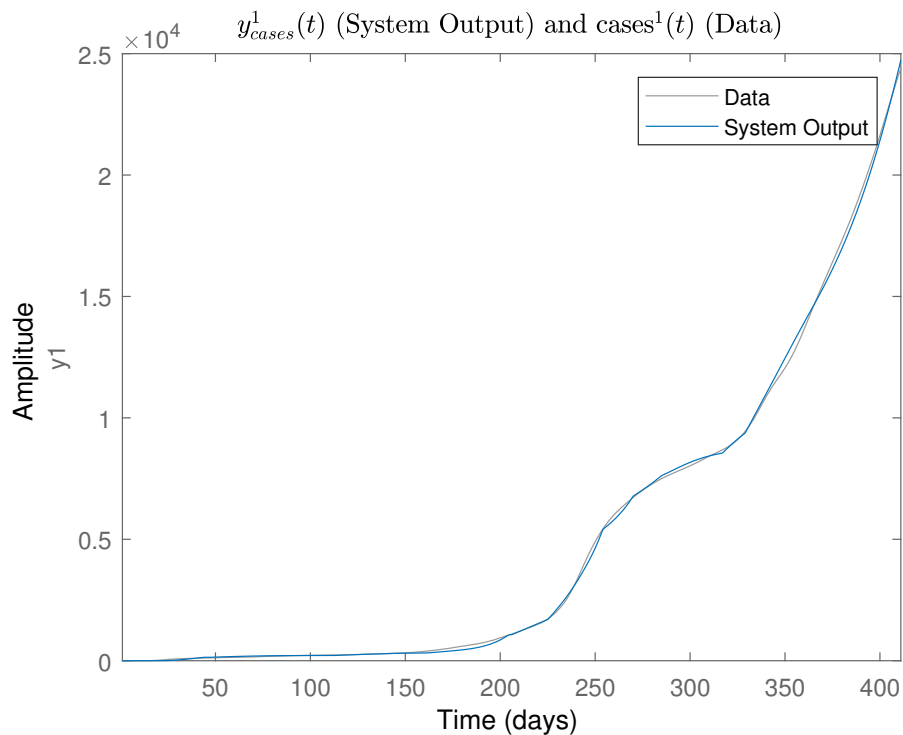
It can be seen that there is an increase in the number of new vaccinated individuals per day  $u^{l,i}(t)$ . This can be explained due to the more vigorous inoculation policy that is adopted by the government.

## 4.3 Fitting the System Outputs to the Measurements

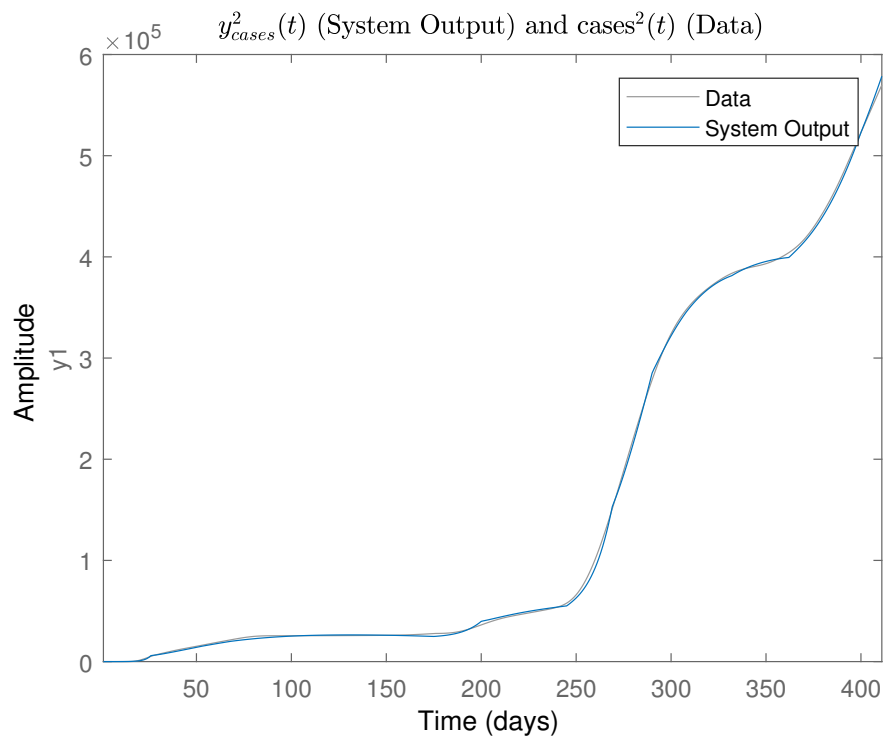
In this section the fitting of the system outputs to the measurements is presented, given the selected values of the parameters of the system, presented in Section 4.2.

### 4.3.1 System Outputs for Cases

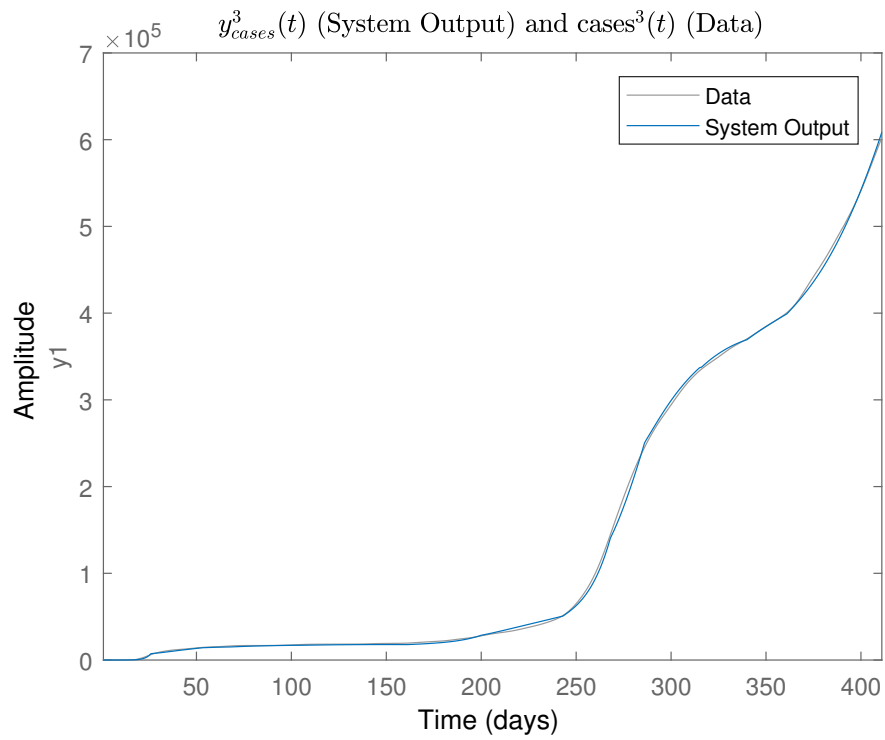
In Figure 4.10, the system outputs  $y_{cases}^i(t)$  are compared to the data cases<sup>i</sup>( $t$ ).



(a)



(b)



(c)

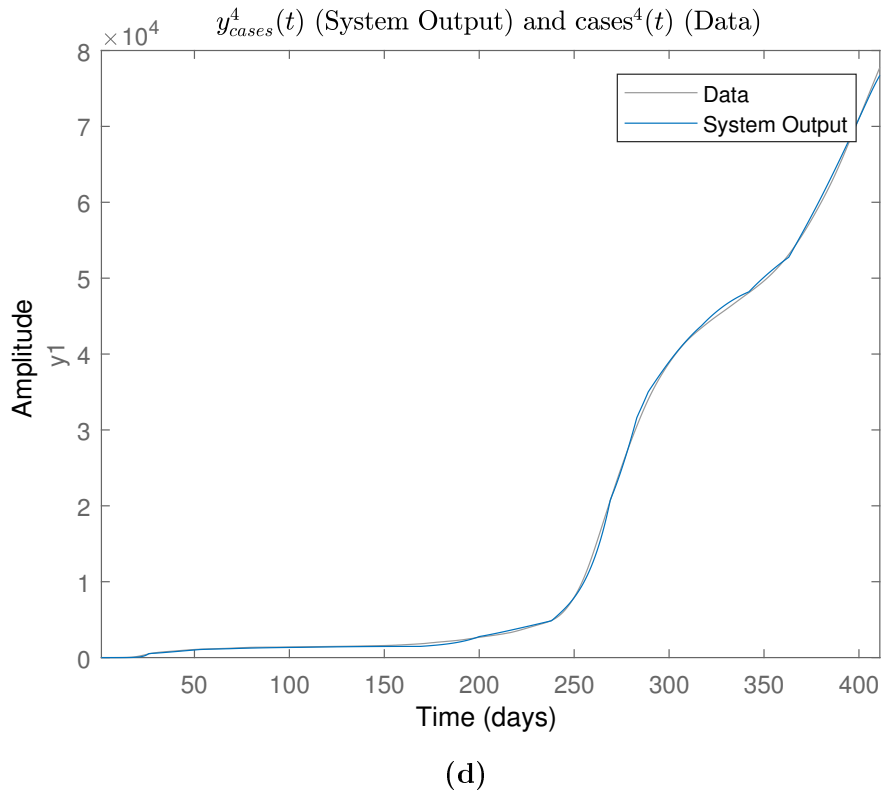


**Figure 4.10:** (a) Fitted curve for new cases at age group 1 (b) fitted curve for new cases at age group 2 (c) fitted curve for new cases at age group 3 (d) fitted curve for new cases at age group 4

The fitness of the system outputs  $y_{cases}^i(t)$  to the data is presented below:

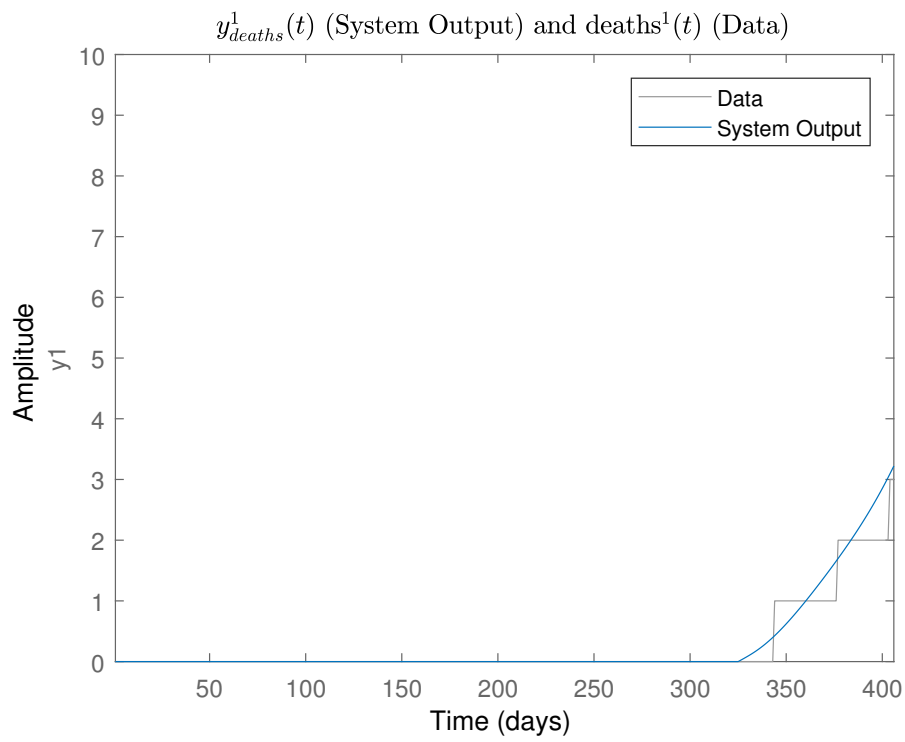
Fitness Value	Age Groups			
	Age Group 1	Age Group 2	Age Group 3	Age Group 4
NRMSE	97.83%	98.62%	98.30%	98.47%

**Table 4.3:** NRMSE percentages for  $y_{cases}^i(t)$ .

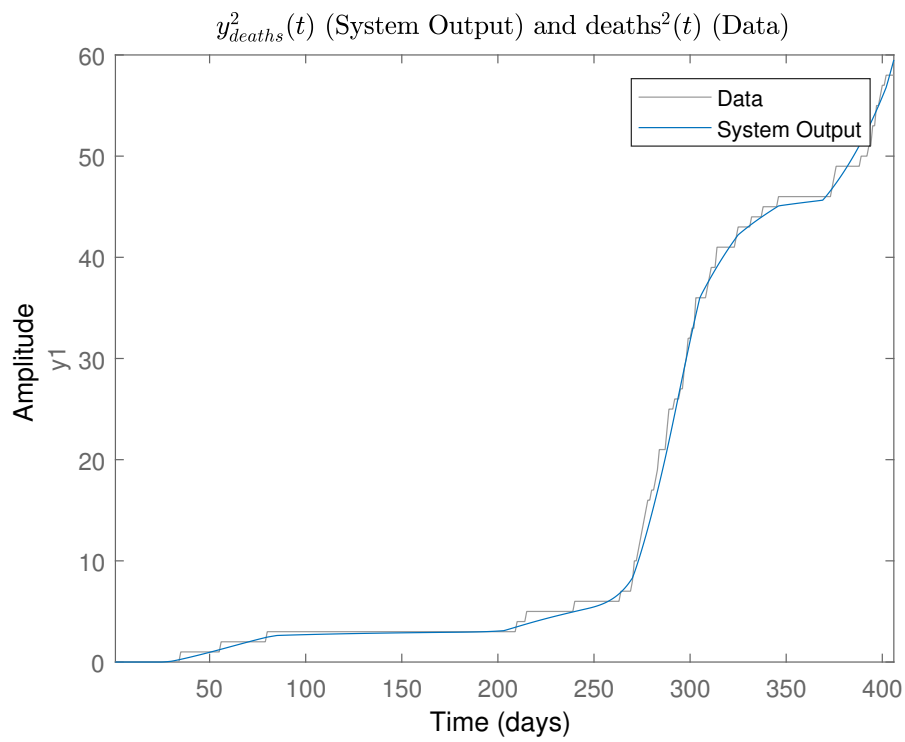
Given the values of the NRMSE measure for  $y_{cases}^i(t)$ , a good fitting has been attained for these system outputs.

### 4.3.2 System Outputs for Deaths

In Fig. 4.11, the system outputs  $y_{deaths}^i(t)$  are compared to the data  $deaths^i(t)$ .



(a)



(b)

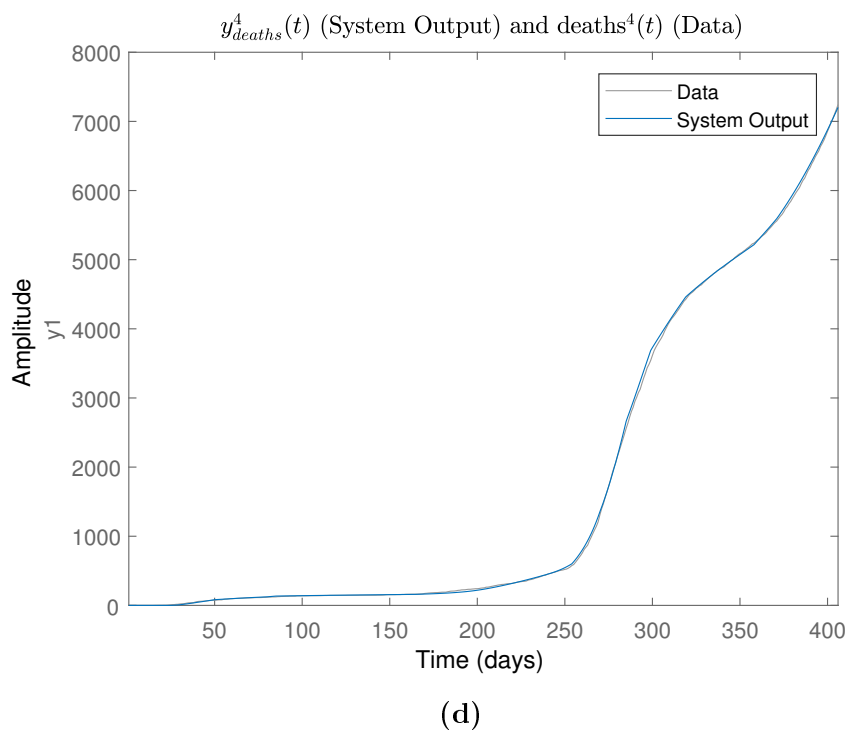
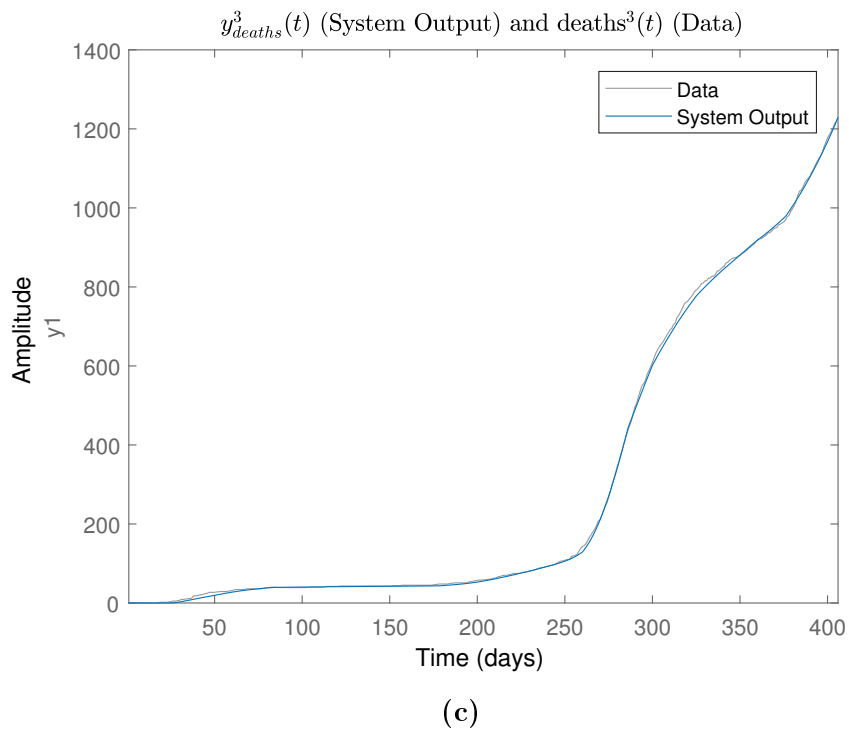


**Figure 4.11:** (a) Fitted curve for deaths at age group 1 (b) fitted curve for deaths at age group 2 (c) fitted curve for deaths at age group 3 (d) fitted curve for deaths at age group 4

The fitness of the system outputs  $y_{\text{deaths}}^i(t)$  to the data is presented below:

Fitness Value	Age Groups			
	Age Group 1	Age Group 2	Age Group 3	Age Group 4
NRMSE	70.50%	96.12%	98.45%	98.67%

**Table 4.4:** NRMSE percentages for  $y_{\text{deaths}}^i(t)$ .

Given the values of the NRMSE measure for  $y_{\text{deaths}}^i(t)$ , a good fitting has been attained for  $i = 2, 3, 4$ . The fitness for  $i = 1$  is substantially worse which can be attributed to the fact that the system outputs are not quantized.

### 4.3.3 System Outputs for Recovered Individuals

In Fig. 4.12, the system outputs  $y_{\text{recovered}}^i(t)$  are compared to the data  $\text{recovered}^i(t)$ .

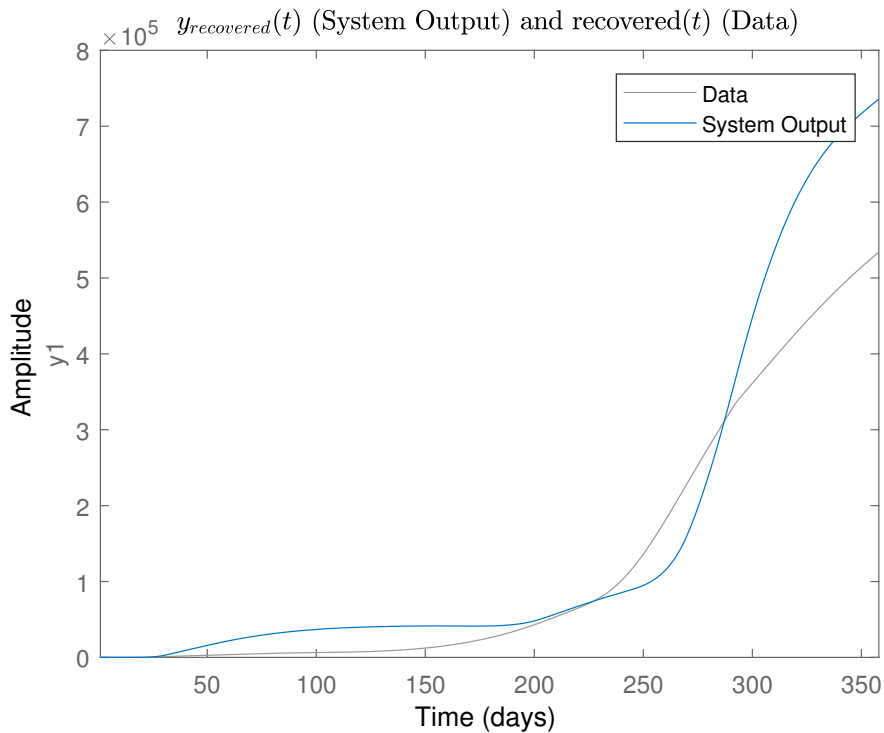


**Figure 4.12:** Fitted curve for recovered individuals

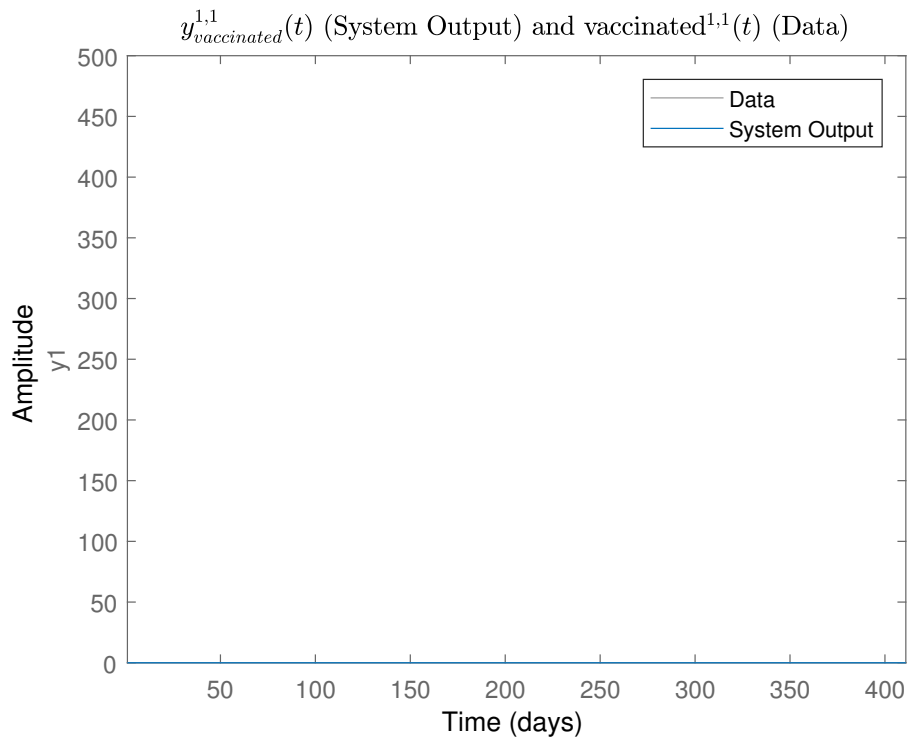
The fitness of the system outputs  $y_{\text{recovered}}(t)$  to the data is 54.42%. As can be seen from Fig. 4.12, the fitting of the output  $y_{\text{recovered}}(t)$  is poor, however this is a desired behavior of the system since the data is merely a prediction of the true number of recovered individuals and not measurements taken from the population.

### 4.3.4 System Outputs for Vaccinated Individuals

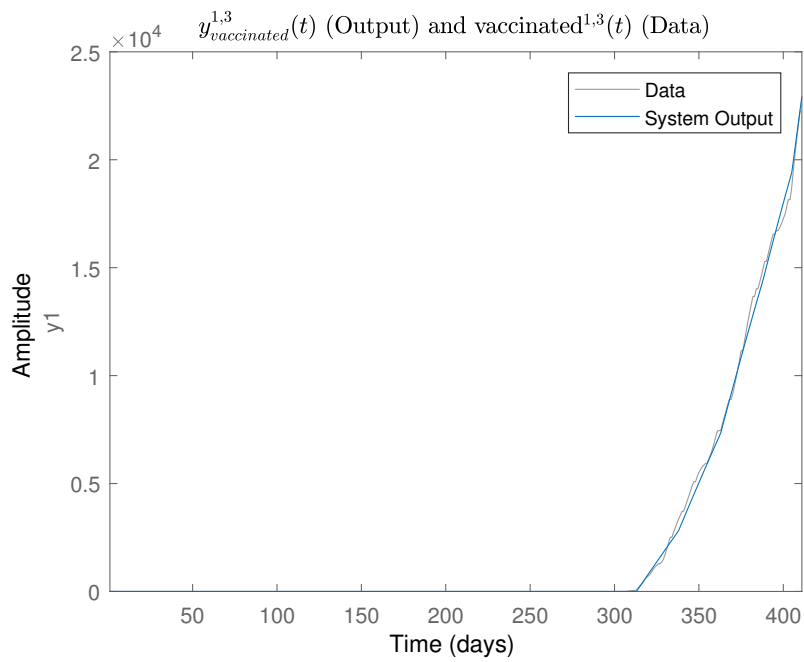
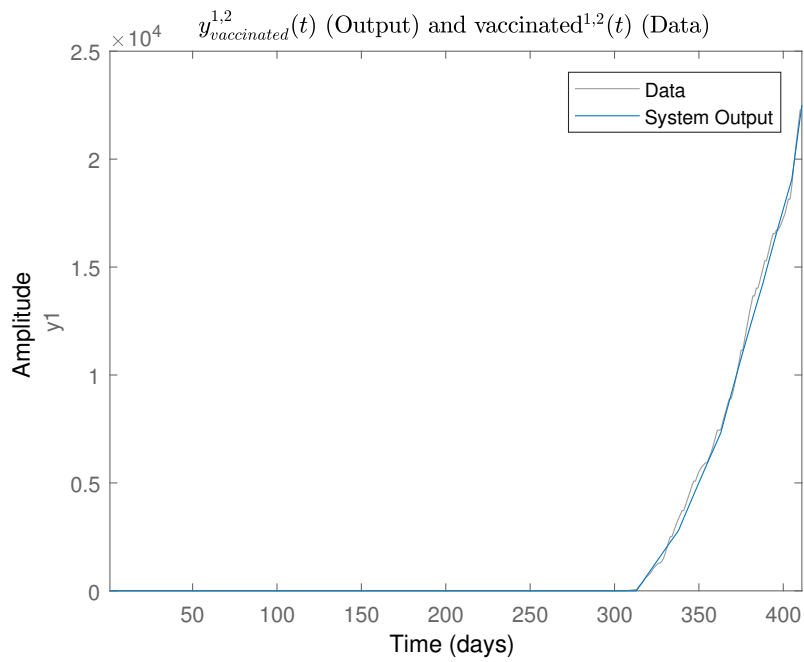
In this paragraph, the fitting of the system outputs  $y_{\text{vaccinated}}^{l,i}(t)$  to their corresponding data is presented.

#### System Outputs $y_{\text{vaccinated}}^{1,i}(t)$

In Fig. 4.13, the system outputs  $y_{\text{cases}}^i(t)$  are compared to the data cases<sup>i</sup>(t).

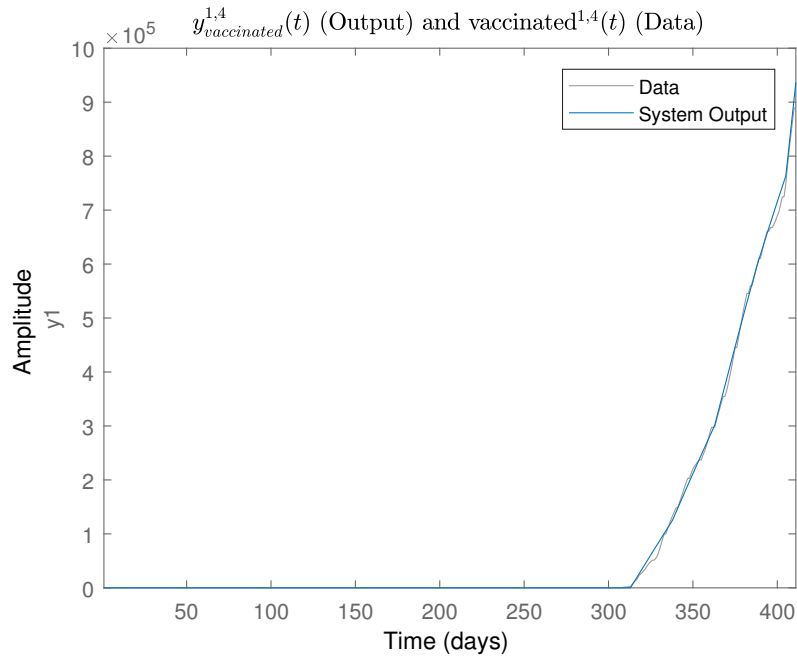


(a)



The fitness percentage of the system outputs  $y^i(t)$  to the data is presented below:

Given the values of the NRMSE measure for  $y_{vaccinated}^{1,i}(t)$ , a good fitting has been attained for all age groups participating in the inoculation strategy.



(d)

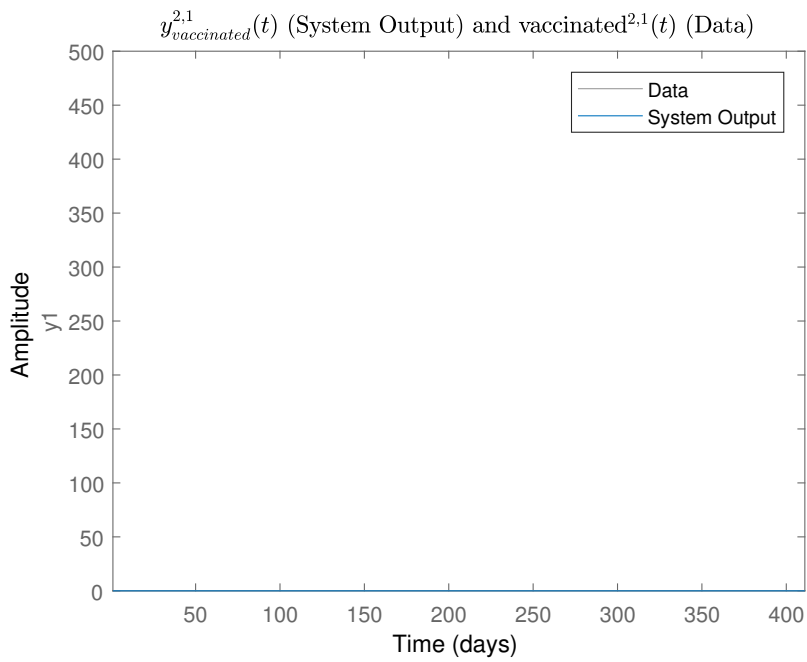
**Figure 4.13:** Fitted curve for vaccinated individuals with vaccine  $l = 1$  at age group: (a)  $i = 1$ , (b)  $i = 2$ , (c)  $i = 3$ , (d)  $i = 4$

Fitness Value	Age Groups			
	Age Group 1	Age Group 2	Age Group 3	Age Group 4
NRMSE	100%	97.09%	96.21%	96.34%

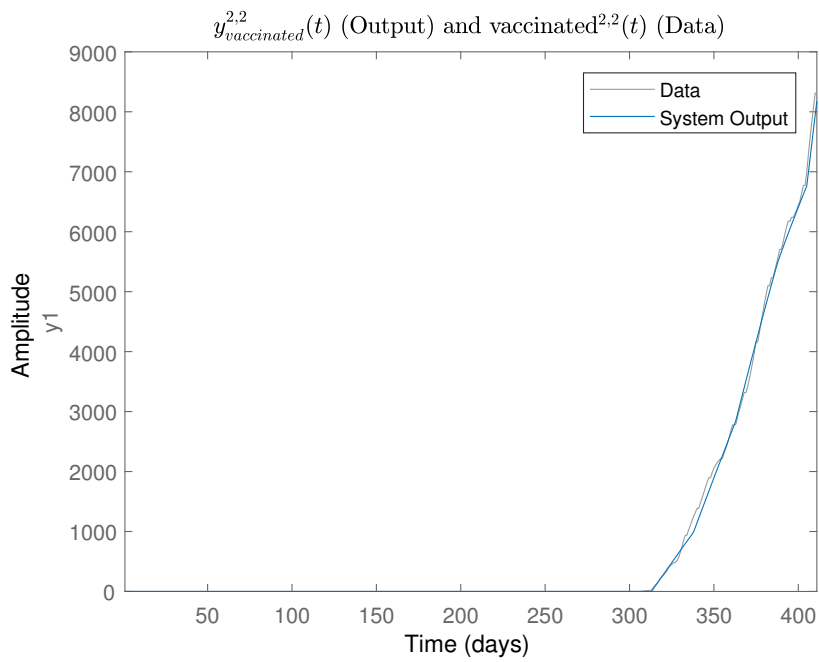
**Table 4.5:** NRMSE percentages for  $y_{\text{vaccinated}}^{1,i}(t)$ .

### System Outputs $y_{\text{vaccinated}}^{2,i}(t)$

In Fig. 4.14, the system outputs  $y_{\text{vaccinated}}^{2,i}(t)$  are compared to the data  $\text{vaccinated}^{2,i}(t)$ .



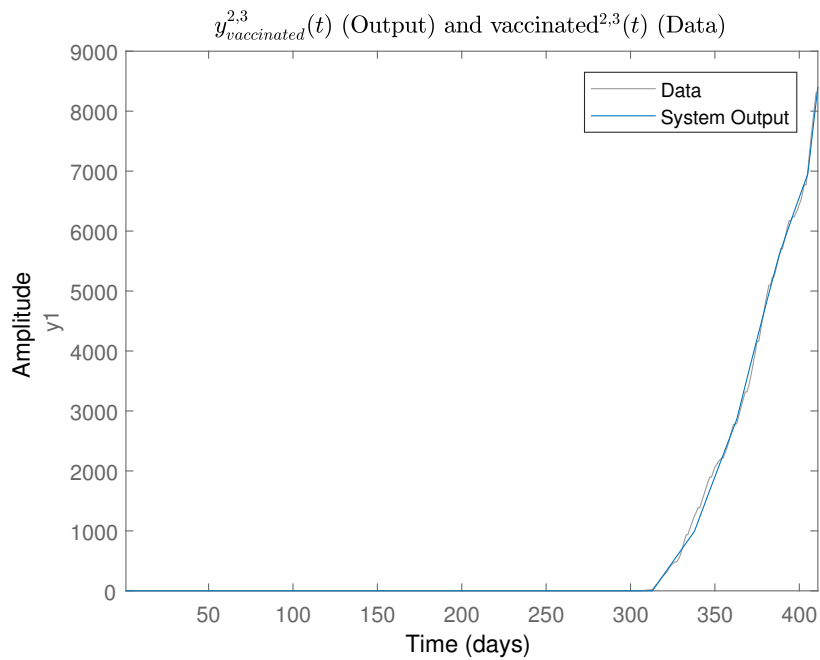
(a)



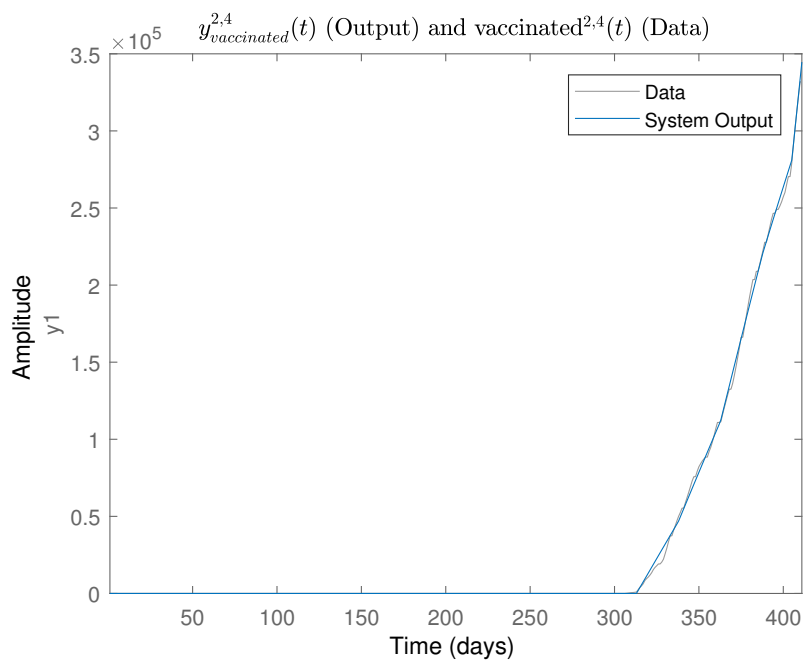
(b)

The fitness of the system outputs  $y_{vaccinated}^{2,i}(t)$  to the data is presented below:

Given the values of the NRMSE measure for  $y_{vaccinated}^{2,i}(t)$ , a good fitting has been attained for all age groups participating in the inoculation strategy.



(c)



(d)

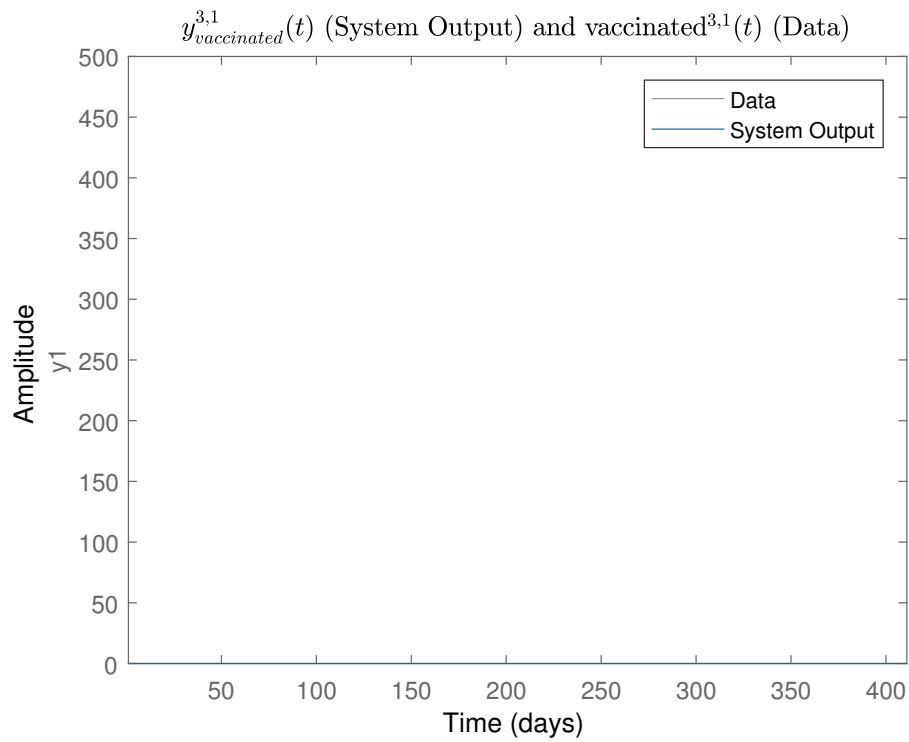
**Figure 4.14:** Fitted curve for vaccinated individuals with vaccine  $l = 2$  at age group: (a)  $i = 1$ , (b)  $i = 2$ , (c)  $i = 3$ , (d)  $i = 4$

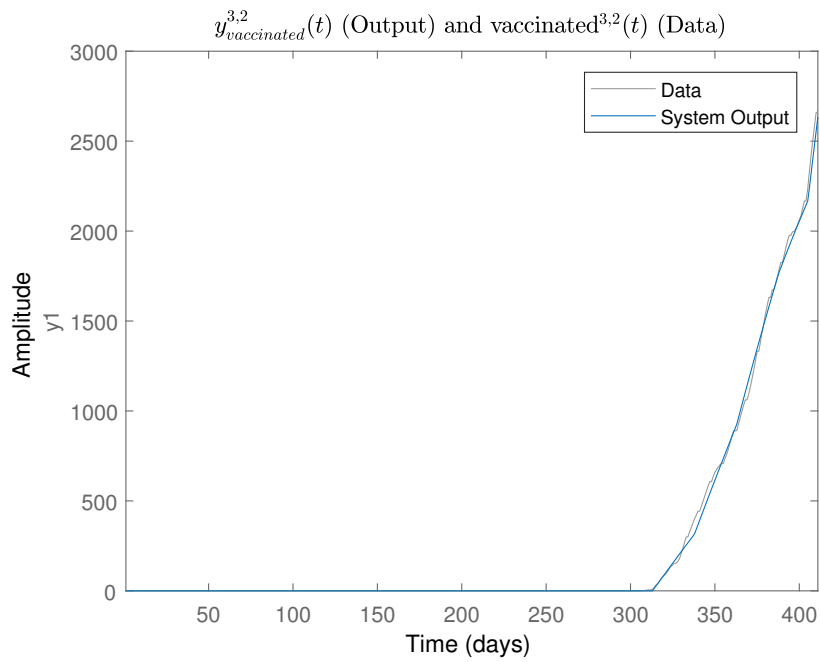
Fitness Value	Age Groups			
	Age Group 1	Age Group 2	Age Group 3	Age Group 4
NRMSE	100%	96.21%	96.95%	97.46%

**Table 4.6:** NRMSE percentages for  $y_{\text{vaccinated}}^{2,i}(t)$ .

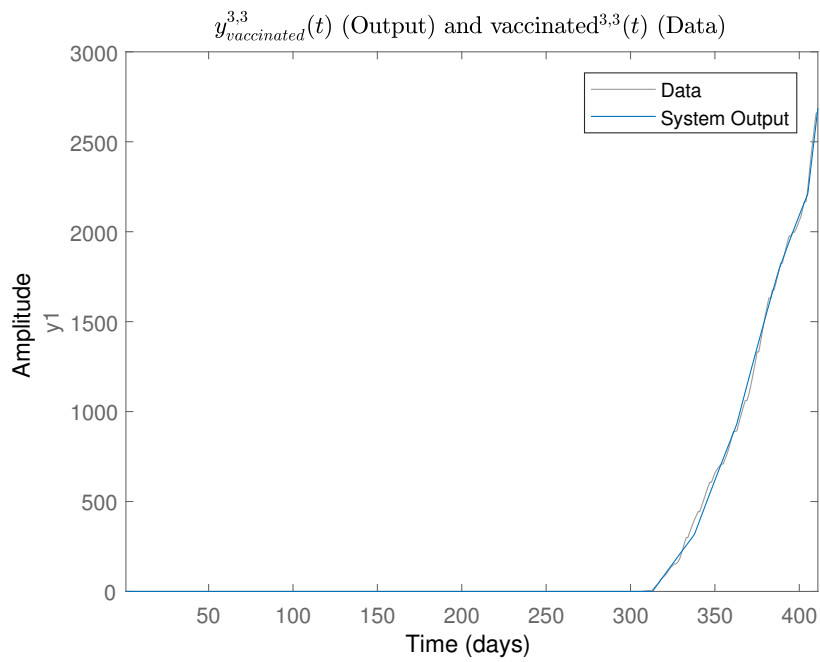
### System Outputs $y_{\text{vaccinated}}^{3,i}(t)$

In Fig. 4.15, the system outputs  $y_{\text{vaccinated}}^{3,i}(t)$  are compared to the data  $\text{vaccinated}^{3,i}(t)$ .





(b)



(c)

The fitness of the system outputs  $y_{vaccinated}^{3,i}(t)$  to the data is presented below:

Given the values of the NRMSE measure for  $y_{vaccinated}^{3,i}(t)$ , a good fitting has been attained for all age groups participating in the inoculation strategy.

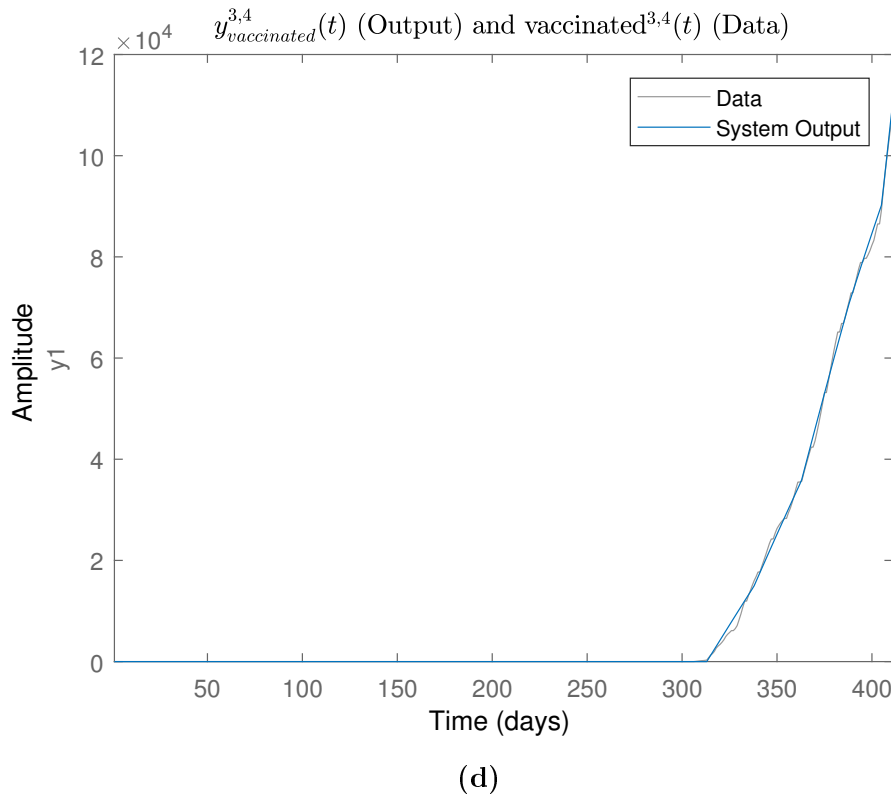


**Figure 4.15:** Fitted curve for vaccinated individuals with vaccine  $l = 3$  at age group: (a)  $i = 1$ , (b)  $i = 2$ , (c)  $i = 3$ , (d)  $i = 4$

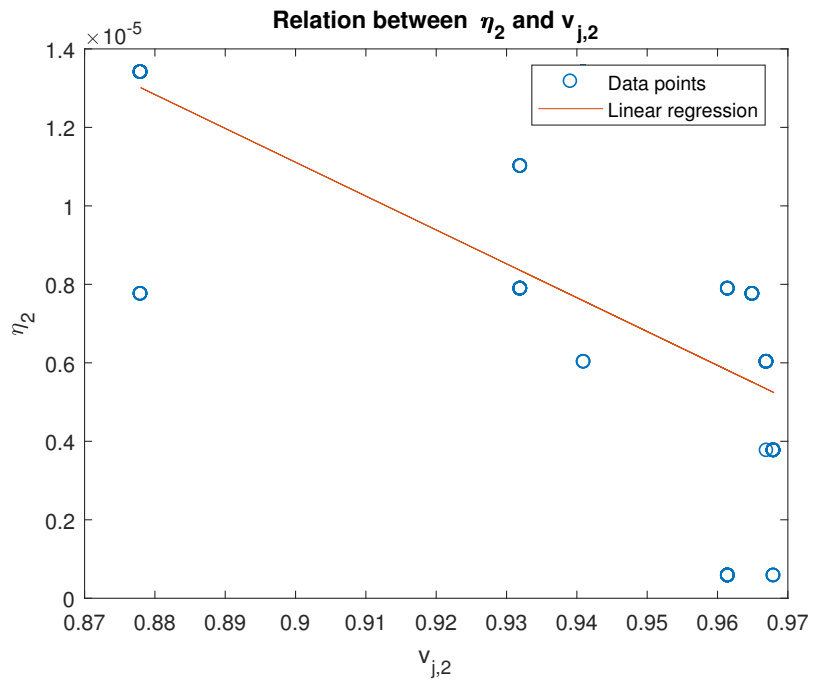
Fitness Value	Age Groups			
	Age Group 1	Age Group 2	Age Group 3	Age Group 4
NRMSE	100%	96.34%	96.8%	97.34%

**Table 4.7:** Final system parameter values for the vaccines.

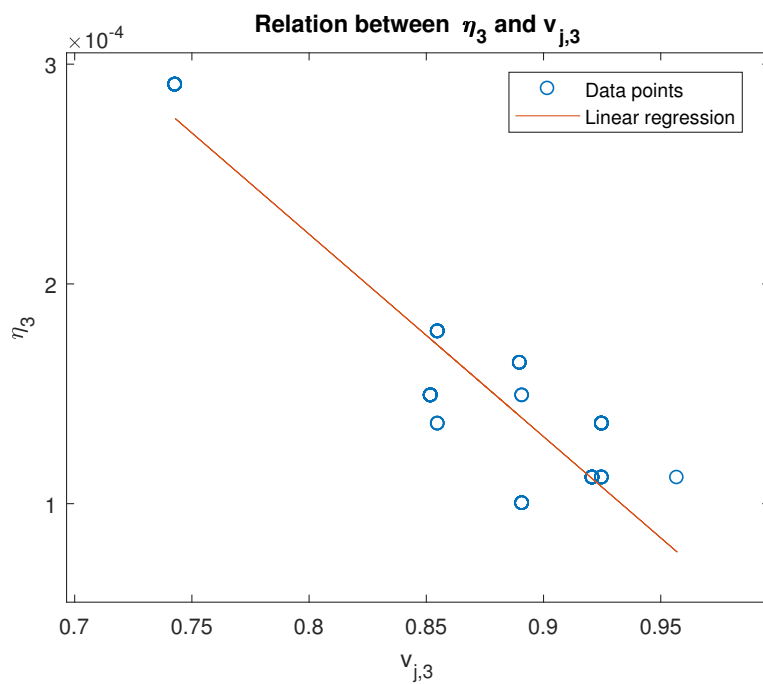
## 4.4 Investigating the Relation between NPI and fatality rates

In order to employ different scenarios for the NPI (e.g. considering a gradual lifting of measures) for future predictions of the pandemic, it may be useful to examine the relation between the NPI measures and the fatality rates. We perform linear regression on data points from the last 4 months. This allows us to estimate the tendencies of the fatality rates under varying NPI measures. It should be noted that, due to the constant values of  $a_{j,i}(t)$  during the second wave, it was not possible to explore how fatality rates are affected by the parameters  $a_{j,i}(t)$  in addition to the NPI measures  $v_{ji}(t)$ .

The results are presented in Fig. 4.16. It can be seen that the NPI measures have a positive effect in the fatality rates.



(a)



(b)

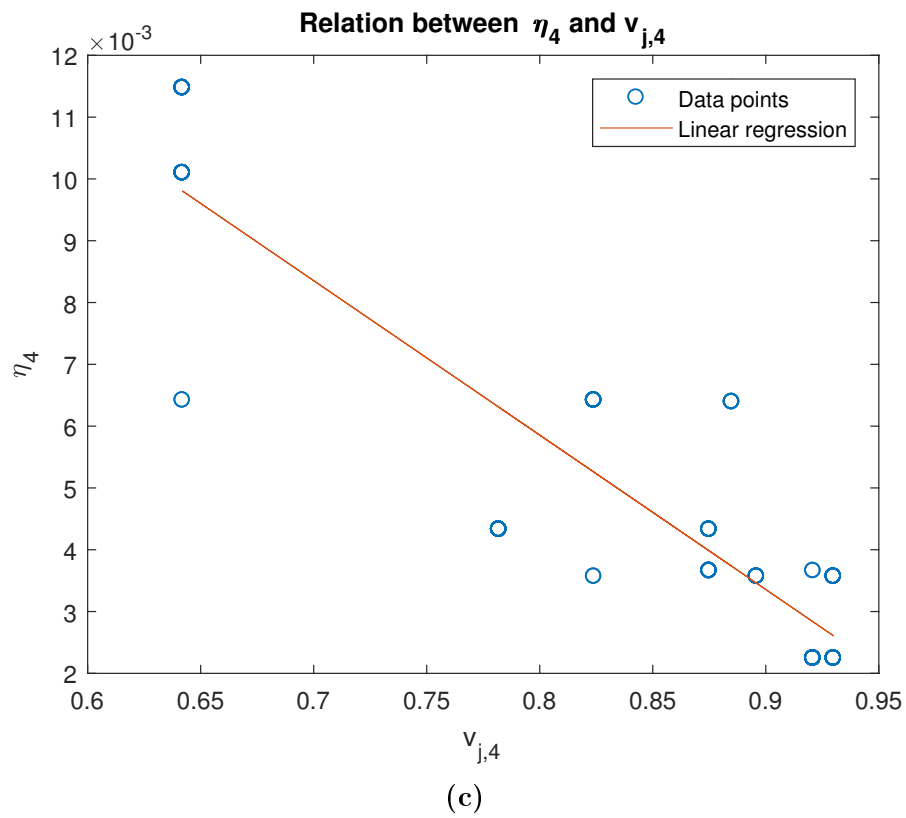


**Figure 4.16:** (a) Linear regression on  $\eta_2$  and  $v_{j,2}$  (b) Linear regression on  $\eta_3$  and  $v_{j,3}$  (c) Linear regression on  $\eta_4$  and  $v_{j,4}$

# Chapter 5

## Pontryagin's Minimum Principle

### 5.1 Introduction

Pontryagin's Minimum Principle provides the system designer with sufficient conditions for an optimal control policy. A controller designed using Pontryagin's Principle is an open-loop controller, that is, no feedback of the system states is presented in the system. This is a logical assumption given the actual inoculation measures taken in a population.

Although originally Pontryagin's Principle seeks to maximize a cost function, in which case the method is called Pontryagin's Maximum Principle, it has been also been extended to solve the problem of minimizing the cost function. In the following Section, Pontryagin's Minimum Principle (which may also be called "Pontryagin's Principle" in this work for simplicity) is presented. Then, Pontryagin's Method is applied on the model and the sufficiency of the conditions imposed is proven.

This work presents the mathematical background for Pontryagin's and the characterization of the optimal controller imposed by the principle. Generally, finding the optimal controller pertains to a Boundary Value Problem (BVP). For systems of high complexity, finding a closed form of the solutions can be an intractable problem due to the boundary constraints. In such cases, the optimal controllers are found by solving the BVP numerically. The results of the application of the optimal inoculation strategy are left as future work for this thesis.

## 5.2 Theoretical Background for Pontryagin's Minimum Principle

Given the nonlinear system

$$\dot{x} = f(x, u), \quad x(0) = x_0, \quad u(t) \in \tilde{U}, \quad (5.1)$$

where  $\tilde{U}$  denotes the *set of admissible control policies*. Define the *cost function*

$$J(x, u) = \int_{t_0}^{t_f} L(x(t), u(t)) dt + \Psi(x(T)) \quad (5.2)$$

where  $\Psi(x(T))$  denotes the *transversality (or terminal) conditions*. [62]

At this point, it is important to introduce the *Hamiltonian* of the control problem:

$$H(x, u, m) := L(x, u, m) + m^\top f(x, u) \quad (5.3)$$

where  $m$  is a vector which contains the adjoint variables for the optimization problem.

Given an optimal control policy,  $u^*(t)$ , one can deduce that  $J(x^*, u^*) \leq J(x_\delta, u_\delta)$  for any admissible control  $u_\delta(t)$  arbitrarily close to the optimal  $u^*(t)$ :

$$\int_{t_0}^{t_f} |u_\delta(t) - u^*(t)| < \epsilon \quad (5.4)$$

for small  $\epsilon$ . However, since the determination of the value of  $J(x_\delta, u_\delta)$  may not always be easy, therefore an alternative (modified) form of the cost function is considered:

$$\tilde{J}(x, u) := J(x, u) - \int_{t_0}^{t_f} m^\top (\dot{x} - f(x, u)) dt = J(x, u) \quad (5.5)$$

Note that the integrand in 5.5 is always zero. The value of the modified cost function is now:

$$\begin{aligned} \tilde{J}(x, u) &:= \Psi(x(t_f)) + \int_{t_0}^{t_f} L(x(t), u(t), m(t)) + m^\top f(x(t), u(t)) dt - \int_{t_0}^{t_f} m(t)^\top \dot{x}(t) dt \\ &= \Psi(x(t_f)) + \int_{t_0}^{t_f} H(x(t), u(t), m(t)) dt - \int_{t_0}^{t_f} m(t)^\top \dot{x}(t) dt \\ &= \Psi(x(t_f)) + \int_{t_0}^{t_f} H(x(t), u(t), m(t)) - m(t)^\top \dot{x}(t) dt \end{aligned} \quad (5.6)$$

Let the optimal control drive the system to the optimal trajectory  $x^*(t)$ . The control  $u_\delta(t)$ , then, drives the system to the "perturbed" optimal trajectory  $x^*(t) + \delta x^*(t)$ . Also, let  $\delta \tilde{J}$  be the corresponding change in the modified cost function. Then, one can deduct:

$$\begin{aligned} \delta \tilde{J} = & \Psi(x^*(t_f) + \delta x^*(t_f)) - \Psi(x^*(t_f)) \\ & + \int_{t_0}^{t_f} H(x^*(t) + \delta x^*(t), u_\delta(t), m(t)) - H(x^*(t), u^*(t), m(t)) - m(t)^\top \delta x dt \end{aligned} \quad (5.7)$$

Integrating  $m(t)^\top \delta x$  by parts, we receive:

$$\begin{aligned} \delta \tilde{J} = & \Psi(x^*(t_f) + \delta x^*(t_f)) - \Psi(x^*(t_f)) + m(0)^\top \delta x(0) - m(t_f)^\top \delta x(t_f) \\ & + \int_{t_0}^{t_f} H(x^*(t) + \delta x^*(t), u_\delta(t), m(t)) - H(x^*(t), u^*(t), m(t)) dt - \int_{t_0}^{t_f} \dot{m}^\top \delta x dt \end{aligned} \quad (5.8)$$

By adding and subtracting  $H(x^*(t), u_\delta(t), m(t))$ , the integral term  $\int_{t_0}^{t_f} H(x^*(t) + \delta x^*(t), u_\delta(t), m(t)) - H(x^*(t), u^*(t), m(t)) dt$  can be written as:

$$\begin{aligned} & \int_{t_0}^{t_f} H(x^*(t) + \delta x^*(t), u_\delta(t), m(t)) - H(x^*(t), u^*(t), m(t)) dt \\ = & \int_{t_0}^{t_f} H(x^*(t) + \delta x^*(t), u_\delta(t), m(t)) - H(x^*(t), u_\delta(t), m(t)) \\ & + H(x^*(t), u_\delta(t), m(t)) - H(x^*(t), u^*(t), m(t)) dt \end{aligned} \quad (5.9)$$

By applying the Taylor series for  $H(x^*(t) + \delta x^*(t), u_\delta(t), m(t)) - H(x^*(t), u_\delta(t), m(t))$  we receive:

$$\begin{aligned} & \int_{t_0}^{t_f} H(x^*(t) + \delta x^*(t), u_\delta(t), m(t)) - H(x^*(t), u^*(t), m(t)) dt \\ = & \int_{t_0}^{t_f} H_x(x^*(t), u_\delta(t), m(t)) \delta x(t) + H(x^*(t), u_\delta(t), m(t)) - H(x^*(t), u^*(t), m(t)) dt + O(\epsilon) \end{aligned} \quad (5.10)$$

Adding and subtracting  $H_x(x^*(t), u^*(t), m(t))\delta x$  in 5.10, we receive:

$$\begin{aligned}
 & \int_{t_0}^{t_f} H(x^*(t) + \delta x^*(t), u_\delta(t), m(t)) - H(x^*(t), u^*(t), m(t)) dt \\
 = & \int_{t_0}^{t_f} H_x(x^*(t), u^*(t), m(t))\delta x(t) + [H_x(x^*(t), u_\delta(t), m(t)) - H_x(x^*(t), u^*(t), m(t))] \delta x(t) \\
 & + H(x^*(t), u_\delta(t), m(t)) - H(x^*(t), u^*(t), m(t)) dt + O(\epsilon)
 \end{aligned} \tag{5.11}$$

The integral  $\int_{t_0}^{t_f} [H_x(x^*(t), u_\delta(t), m(t)) - H_x(x^*(t), u^*(t), m(t))] \delta x(t) dt$  is of order  $\epsilon^2$ , therefore 5.11 becomes:

$$\begin{aligned}
 & \int_{t_0}^{t_f} H(x^*(t) + \delta x^*(t), u_\delta(t), m(t)) - H(x^*(t), u^*(t), m(t)) dt \\
 = & \int_{t_0}^{t_f} H_x(x^*(t), u^*(t), m(t))\delta x(t) + H(x^*(t), u_\delta(t), m(t)) - H(x^*(t), u^*(t), m(t)) dt \\
 & + O(\epsilon) + O(\epsilon^2)
 \end{aligned} \tag{5.12}$$

By denoting  $O'(\epsilon)$  all the terms of order  $\epsilon$  or lower, 5.12 becomes:

$$\begin{aligned}
 & \int_{t_0}^{t_f} H(x^*(t) + \delta x^*(t), u_\delta(t), m(t)) - H(x^*(t), u^*(t), m(t)) dt \\
 = & \int_{t_0}^{t_f} H_x(x^*(t), u^*(t), m(t))\delta x(t) + H(x^*(t), u_\delta(t), m(t)) - H(x^*(t), u^*(t), m(t)) dt \\
 & + O'(\epsilon)
 \end{aligned} \tag{5.13}$$

Substituting Eq. (5.13) in Eq. (5.8) and applying the Taylor expansion for  $\Psi(x^*(t_f) + \delta x^*(t_f)) - \Psi(x^*(t_f))$ , we obtain the following expression for the change in the modified cost function:

$$\begin{aligned}
 \delta \tilde{J} = & [\Psi_x(x^*(t_f)) - m^\top(t_f)] \delta x(t_f) - m(0)^\top \delta x(0) \\
 & + \int_{t_0}^{t_f} [H_x(x^*(t), u^*(t), m(t)) - \dot{m}^\top(t_f)] \delta x(t) dt \\
 & + \int_{t_0}^{t_f} H(x^*(t), u_\delta(t), m(t)) - H(x^*(t), u^*(t), m(t)) dt + O'(\epsilon)
 \end{aligned} \tag{5.14}$$

Moreover, considering  $O'(\epsilon) \rightarrow 0$ , we can approximate  $\delta\tilde{J}$  as:

$$\begin{aligned} \delta\tilde{J} &\approx [\Psi_x(x^*(t_f)) - m^\top(t_f)]\delta x(t_f) - m(0)^\top\delta x(0) \\ &\quad + \int_{t_0}^{t_f} [H_x(x^*(t), u^*(t), m(t)) - \dot{m}^\top(t_f)]\delta x(t)dt \\ &\quad + \int_{t_0}^{t_f} H(x^*(t), u_\delta(t), m(t)) - H(x^*(t), u^*(t), m(t))dt \end{aligned} \quad (5.15)$$

The expression from Eq. (5.18) can be further simplified, given that  $\delta x(0) = 0$  since the control does not affect the system states at  $t = 0$  and by assuming:

$$m^\top(t_f) = \Psi_x(x^*(t_f)) \quad (5.16)$$

$$-\dot{m}^\top(t) = H_x(x^*(t), u^*(t), m(t)) \quad (5.17)$$

Thus, Eq. (5.18) becomes:

$$\delta\tilde{J} \approx \int_{t_0}^{t_f} H(x^*(t), u_\delta(t), m(t)) - H(x^*(t), u^*(t), m(t))dt \quad (5.18)$$

In order for  $u^*(t)$  to be optimal,  $\delta\tilde{J}$  needs to be positive, that is,  $\delta\tilde{J} > 0$ . This can be achieved by demanding the following condition:

$$H(x^*(t), u^*(t), m(t)) \leq H(x^*(t), u_\delta, m(t)), \text{ for all } t \in [t_0, t_f] \text{ and } u_\delta \in \tilde{U} \quad (5.19)$$

Eq. (5.16), Eq. (5.17), Eq. (5.19) define the necessary conditions for Pontryagin's Minimum Principle.

In this work, the case of fixed final time  $t_f$  and free terminal states  $\mathbf{x}(t_f)$  have been considered. These assumptions may naturally hold true for an inoculation strategy. For example, it might be more important to achieve a specific threshold of immunizations in the population, either as a total or per each age-group, than demanding the system states to attain a specific value at  $t = t_f$ . Moreover, as will be explained later in more detail, it might be needed that a vaccination strategy run on a specific time frame (for example, attain a percentage of 75% of individuals by the beginning of September).

## 5.3 Application of Pontryagin's Principle in the System with Control

### 5.3.1 Formulation of the Optimal Control Problem

Given the system with controls defined in Section 1.2.2, we define the following cost function:

$$J(\mathbf{x}(t), \mathbf{u}(t)) = \Psi(\mathbf{x}(t_f)) + \int_{t_0}^{t_f} \sum_{i=1}^4 D^i(t) + \mathbf{u}^\top(t) \mathbf{R} \mathbf{u}(t) dt \quad (5.20)$$

where  $\mathbf{R}$  is a positive definite diagonal matrix denoting the weights for the control variables and the terminal function  $\Psi(\mathbf{x}(T))$  are defined as:

$$\Psi(\mathbf{x}(t_f)) = \left\{ N^* - \sum_i [R^i(t_f) + V_+^i(t_f)] \right\}^2 \quad (5.21)$$

where  $N^*$  is the target number of individuals to be immune to the virus. In this work,  $N^*$  is considered equal to  $\left(1 - \frac{1}{R_0}\right)N$ , for which herd immunity can be achieved. We define the set of all admissible control policies  $\tilde{U} = \{\mathbf{u}(t) \in \mathbb{R}^m : 0 \leq u^{l,i}(t) \leq u_{\max}^{l,i}\}$ . The optimal control policy is denoted by  $\mathbf{u}^*(t)$  and minimizes the cost function presented in Eq. (5.41).

### 5.3.2 Existence of Optimal Control

The following Lemma and its proof are given for the problem of minimization of Eq. (5.41):

**Lemma 5.3.1.** *The optimal solution exists for the optimal control problem defined in Section 5.3.1.*

*Proof.* From Theorem 4.1 of [63], the following conditions must hold for the existence of the optimal control:

1. the set of solutions for the system,  $F$ , is non-empty,
2. the set  $\tilde{U}$  is closed,
3. the set of end-conditions,  $S$ , is compact and  $\Psi(\cdot)$  is continuous in  $S$ ,

4. the set  $\tilde{U}$  is convex, the system is given in the control-affine form and the objective function  $L(\mathbf{x}(t), \mathbf{u}(t))$  is convex on  $\tilde{U}$ ,
5.  $L(\mathbf{x}(t), \mathbf{u}(t)) \geq c_1 \|\mathbf{u}(t)\|^n - c_2$ ,  $c_1 > 0$ ,  $n > 1$ .

Condition 1. can easily be proven. From [64], since  $\mathbf{f}(\mathbf{x}(t), \mathbf{u}(t))$  is continuous (or piece-wise continuous), then there exists a solution  $\mathbf{x}(t)$  for the system.

Conditions 2. and 4. can also be easily proven. Given that  $\tilde{U} = \{\mathbf{u}(t) : 0 \leq u^{l,i}(t) \leq u_{\max}^{l,i}\} = [0, u_{\max}^{1,1}] \times \dots \times [0, u_{\max}^{k_v,1}] \times \dots \times [0, u_{\max}^{1,4}] \times \dots \times [0, u_{\max}^{k_v,4}]$ , it is easy to see that it is closed and convex. From Section 1.2.2 it has been shown that the system with control is in the affine in the control form.

Condition 3. can be proven by inferring boundedness of the system states for the system with control. The system states in Eq. (1.2.2) are bounded from below and from above, since no demographics have been considered in the model, that is,  $0 \leq k^i(t) \leq N_i$  for  $k = \{S, E, I, R, D\}$  and  $0 \leq k^{l,i}(t) \leq N_i$  for  $k = \{V_-, V_+\}$ . The set of end-conditions  $S$  is defined as

$$S = \{\mathbf{x}(t_f) : 0 \leq k^i(t) \leq N_i \text{ for } k = \{S, E, I, R, D\} \text{ and } 0 \leq k^{l,i}(t) \leq N_i \text{ for } k = \{V_-, V_+\}\} \quad (5.22)$$

for which one can see that it is compact and that  $\Psi(\mathbf{x}(t_f))$  is continuous with respect to  $\mathbf{x}(t_f)$ .

Condition 5. can be proven by using an upper bound on the quadratic form of  $\mathbf{u}(t)$ :

$$L(\mathbf{x}(t), \mathbf{u}(t)) = D^i(t) + \mathbf{u}^\top(t) \mathbf{R} \mathbf{u}(t) \geq \lambda_{\min}(\mathbf{R}) \|\mathbf{u}(t)\|^2 \quad (5.23)$$

where  $\lambda_{\min}(\mathbf{R}) > 0$  denotes the smallest eigenvalue of  $\mathbf{R}$ .

This completes the proof of the Lemma.  $\square$

Having proven the existence of the optimal controller, we may now turn our focus on characterizing the optimal controller  $\mathbf{u}^*(t)$ .

### 5.3.3 Characterizing the Optimal Controller

Let us propose the following Theorem for the optimal control problem:

**Theorem 5.3.2.** *Consider the optimal control problem in Section 5.3.1. Let the vector of costate equations  $\mathbf{m}(t)$  and  $\mathbf{u}(t) \in \tilde{U}$  with components  $u^{l,i}(t)$  which satisfies:*

$$u^{l,i}(t) = \begin{cases} 0 & \phi^{l,i}(t) \leq 0 \\ \phi^{l,i}(t) & 0 \leq \phi^{l,i}(t) < u_{max}^{l,i} \\ u_{max}^{l,i} & u_{max}^{l,i} \leq \phi^{l,i}(t) \end{cases}$$

where  $\phi^{l,i}(t) := \frac{1}{2}r_{idx,idx}^{-1} [m_{V_-}^{l,i}(t) - m_S^i(t)]$  with  $idx = 4(i-1) + l$ , and  $\mathbf{m}(t)$  is the vector of adjoint variables (costates) which satisfies the adjoint equations and the adjoint final conditions imposed by Pontryagin's Minimum Principle. Given that the system states are bounded, the control policy  $\mathbf{u}(t)$  is optimal for  $t_f$  sufficiently small.

*Proof.* The cost function  $J(\mathbf{x}(t), \mathbf{u}(t))$  and the optimal control problem are defined in Section 5.3. From Lemma 5.3.1, it is inferred that the system has an optimal controller in the set of admissible controllers  $\tilde{U}$ .

Also, define the costate variables  $\mathbf{m}(t)$ , each component of which pertains to a system state. Let us denote each component of  $\mathbf{m}(t)$  as  $m_k^i(t)$ , for  $k \in \{S, E, I, R, D\}$  and  $m_k^{l,i}(t)$ , for  $k \in \{V_-, V_+\}$ .

It should be noted that direct application of Pontryagin's Minimum Principle can lead to the violation of the constraints  $S^i(t) \geq 0$ . Therefore, in addition to the system's dynamical equations considered in the Hamiltonian, the constraints  $S^i(t) \geq 0$  will have to be accounted for. Thus, we define the augmented system states  $\bar{\mathbf{x}}(t)$  and costates  $\bar{\mathbf{m}}(t)$ .

$$\bar{\mathbf{x}}(t) = [\mathbf{x}^\top(t) \quad x_{sc}(t)]^\top \tag{5.24}$$

$$\bar{\mathbf{m}}(t) = [\mathbf{m}^\top(t) \quad m_{sc}(t)]^\top \tag{5.25}$$

where  $x_{sc}(t)$  satisfies:

$$\begin{aligned} \dot{x}_{sc}(t) &= f_{sc}(t, \mathbf{x}(t), \mathbf{u}(t)) = \sum_i [S^i(t)]^2 \mathbb{1}(-S^i(t)), \\ x_{sc}(t_0) &= x_{sc}(t_f) = 0 \end{aligned} \tag{5.26}$$

The Hamiltonian function of the optimization problem is defined as:

$$H(\mathbf{x}(t), \mathbf{u}(t), \mathbf{m}(t)) = \sum_{i=1}^4 D^i(t) + \mathbf{u}^\top(t) \mathbf{R} \mathbf{u}(t) + \bar{\mathbf{m}}^\top(t) \mathbf{f}(t, \mathbf{x}(t), \mathbf{u}(t)) \tag{5.27}$$

where

$$\begin{aligned} \bar{\mathbf{m}}^\top(t) \mathbf{f}(t, \mathbf{x}, \mathbf{u}) = & \sum_i \left[ \sum_n m_n^i(t) f_n^i(t, \mathbf{x}, \mathbf{u}) + \sum_{\hat{n}} \sum_l m_{\hat{n}}^{l,i}(t) f_{\hat{n}}^{l,i}(t, \mathbf{x}, \mathbf{u}) \right] \\ & + m_{\text{sc}}(t) f_{\text{sc}}(t, \mathbf{x}, \mathbf{u}), \quad n \in \{S, E, I, R, D\}, \hat{n} \in \{V_-, V_+\} \end{aligned} \quad (5.28)$$

Let us now examine the Hessian matrix of the Hamiltonian function  $H(\mathbf{x}, \mathbf{u}, \mathbf{m}(t))$ :

$$\frac{\partial^2 H}{\partial \mathbf{u}^2}(\mathbf{x}(t), \mathbf{u}(t), \mathbf{m}(t)) = 2 \begin{bmatrix} r_{1,1} & 0 & \dots & 0 \\ 0 & r_{2,2} & \dots & 0 \\ \vdots & \vdots & \ddots & 0 \\ 0 & 0 & \dots & r_{m,m} \end{bmatrix} = 2\mathbf{R} > 0 \quad (5.29)$$

as can be seen from Eq. (5.52), the Hessian matrix  $\frac{\partial^2 H}{\partial \mathbf{u}^2}(\mathbf{x}(t), \mathbf{u}(t), \mathbf{m}(t))$  is positive definite, meaning that the Hamiltonian function  $H(\mathbf{x}(t), \mathbf{u}(t), \mathbf{m}(t))$  is strictly convex for all control variables  $u^{l,i}(t)$ .

From the adjoint final time conditions in Eq. (5.16), we have:

$$\begin{aligned} m_S^i(t_f) = m_E^i(t_f) = m_I^i(t_f) = m_D^i(t_f) = m_{V_-}^{l,i}(t_f) = 0, \\ m_R^i(t_f) = m_{V_+}^{l,i}(t_f) = -2 \left[ N^* - \sum_i (R^i(t_f) + V_+^i(t_f)) \right] \end{aligned} \quad (5.30)$$

From the necessary condition in Eq. (5.17), we have:

$$\begin{aligned} -\dot{m}_S^i(t) &= -\lambda^i(t, \mathbf{I}(t)) m_S^i(t) + \lambda^i(t, \mathbf{I}(t)) m_E^i(t) + \frac{\partial f_{\text{sc}}^i}{\partial S^i}(t, \mathbf{x}(t), \mathbf{u}(t)) m_{\text{sc}}(t) \\ -\dot{m}_E^i(t) &= -\sigma_i m_E^i(t) + \sigma_i m_I^i(t) \\ -\dot{m}_I^i(t) &= -\left[ \gamma_i + \eta_i(t) - \frac{a_{i,i}(t)}{N_i} (1 - v_{i,i}(t)) S^i(t) \right] m_I^i(t) + \gamma_i m_R^i(t) + \eta_i(t) m_D^i(t) \\ -\dot{m}_R^i(t) &= -\xi_i m_R^i(t) + \xi_i m_S^i(t) \\ -\dot{m}_{V_-}^{l,i}(t) &= -\left[ \lambda^i(t, \mathbf{I}(t)) + \rho_l \frac{w_b^{l,i}}{\tau_l} \right] m_{V_-}^{l,i}(t) + \lambda^i(t, \mathbf{I}(t)) m_E^i(t) + \rho_l \frac{w_b^{l,i}}{\tau_l} m_S^i(t) \\ -\dot{m}_{V_+}^{l,i}(t) &= -\psi_i m_{V_+}^{l,i}(t) + \psi_i m_S^i(t) \\ -\dot{m}_D^i(t) &= 1 \\ -\dot{m}_{\text{sc}}(t) = 0 &\implies m_{\text{sc}}(t) = c \neq 0 \end{aligned} \quad (5.31)$$

From the necessary condition in Eq. (5.19), the optimal control  $\mathbf{u}(t)$  with

elements  $u^{l,i}(t)$  must satisfy:

$$\mathbf{u}^*(t) = \arg \min_{\mathbf{u}(t) \in \tilde{U}} H(\mathbf{x}(t), \mathbf{u}(t), \mathbf{m}(t)) \quad (5.32)$$

We can find the  $\mathbf{u}(t)$  which minimizes the Hamiltonian by solving:

$$\frac{\partial H}{\partial u^{l,i}}(\mathbf{x}(t), \mathbf{u}(t), \mathbf{m}(t)) = 0 \quad (5.33)$$

Let us now define the indicator functions  $\phi^{l,i}(t)$  [65] for each component  $u^{l,i}(t)$  of  $\mathbf{u}(t)$  as the solution to Eq. (5.33):

$$\phi^{l,i}(t) := \frac{1}{2} r_{\text{idx}, \text{idx}}^{-1} [m_{V_-}^{l,i}(t) - m_S^i(t)] \quad (5.34)$$

where  $\text{idx}$  denotes the row and column index of  $\mathbf{R}$  for the element that is the optimization weight of the control variable  $u^{l,i}(t)$  and is defined as:

$$\text{idx}(l, i) := 4(i - 1) + l \quad (5.35)$$

Given that the optimal solution exists and that it satisfies Eq. (5.51), we notice that the first derivative of the Hamiltonian is a linear function with respect to the control variable  $u^{l,i}(t)$ . Thus, the stationary point of the Hamiltonian is unique and therefore is a global minimum for the Hamiltonian.

The value for each control variable in  $\mathbf{u}(t)$  is then given by:

$$\begin{aligned} u^{l,i}(t) &= \max \{0, \min\{u_{\max}^{l,i}, \phi^{l,i}(t)\}\} \\ \iff u^{l,i}(t) &= \begin{cases} 0 & \phi^{l,i}(t) \leq 0 \\ \phi^{l,i}(t) & 0 \leq \phi^{l,i}(t) \leq u_{\max}^{l,i} \\ u_{\max}^{l,i} & u_{\max}^{l,i} \leq \phi^{l,i}(t) \end{cases} \end{aligned} \quad (5.36)$$

Generally, the sufficiency of Pontryagin's Minimum principle cannot be established if certain conditions do not hold true. This is explored later in Theorem 5.3.3. For bounded system states  $\mathbf{x}(t)$ , however, it can be proven that for sufficiently small  $t_f$ , the optimality system  $[\bar{\mathbf{x}}(t) \quad \bar{\mathbf{m}}(t)]$  has a unique solution. The proof is analogous to the ones presented in [66, 67]. Uniqueness of the solution of the optimality system implies in turn uniqueness of the admissible controller  $\mathbf{u}(t)$  that satisfies Pontryagin's Minimum Principle Conditions.

Then, for  $t_f$  sufficiently small, the control  $\mathbf{u}(t)$ , with components given by Eq.

(5.55), is the optimal control policy  $\mathbf{u}^*(t)$ :

$$\begin{aligned} u_*^{l,i}(t) &\equiv \max \{0, \min\{u_{\max}^{l,i}, \phi^{l,i}(t)\}\} \\ \iff u_*^{l,i}(t) &= \begin{cases} 0 & \phi^{l,i}(t) \leq 0 \\ \phi^{l,i}(t) & 0 \leq \phi^{l,i}(t) \leq u_{\max}^{l,i} \\ u_{\max}^{l,i} & u_{\max}^{l,i} \leq \phi^{l,i}(t) \end{cases} \end{aligned} \quad (5.37)$$

where

$$\phi^{l,i}(t) := \frac{1}{2} r_{\text{idx}, \text{idx}}^{-1} [m_{V_-}^{l,i}(t) - m_S^i(t)] \quad (5.38)$$

This completes the proof of the Theorem.  $\square$

In the following theorem, an optimal controller will be provided for the optimization problem in Section 5.3.1 expressed in the Mayer form. Under convexity conditions of the functional  $\mathbf{u} \mapsto \Psi(\mathbf{x}(t_f, \mathbf{u}))$ , the necessary conditions imposed by Pontryagin's Minimum Principle become sufficient.

**Theorem 5.3.3.** *Consider the optimal control problem in Section 5.3.1. Assume that the mapping  $\mathbf{u} \mapsto \Psi(\mathbf{x}(t_f, \mathbf{u}))$  is convex in the control  $\mathbf{u}$ . Let the vector of costate equations  $\mathbf{m}(t)$  and  $\mathbf{u}(t) \in \tilde{U}$  with components  $u^{l,i}(t)$  which satisfies:*

$$u^{l,i}(t) = \begin{cases} 0 & \phi^{l,i}(t) \leq 0 \\ \phi^{l,i}(t) & 0 \leq \phi^{l,i}(t) < u_{\max}^{l,i} \\ u_{\max}^{l,i} & u_{\max}^{l,i} \leq \phi^{l,i}(t) \end{cases}$$

where  $\phi^{l,i}(t) := \frac{1}{2} r_{\text{idx}, \text{idx}}^{-1} [m_{V_-}^{l,i}(t) - m_S^i(t)]$  with  $\text{idx} = 4(i-1) + l$ , and  $\mathbf{m}(t)$  is the vector of adjoint variables (costates) which satisfies the adjoint equations and the adjoint final conditions imposed by Pontryagin's Minimum Principle. The control policy  $\mathbf{u}(t)$ , which satisfies Pontryagin's Minimum Principle, is optimal.

*Proof.* Let the cost function to be minimized from Section 5.3.1:

$$J(\mathbf{x}(t), \mathbf{u}(t)) = \Psi(\mathbf{x}(t_f)) + \int_{t_0}^{t_f} \sum_{i=1}^4 D^i(t) + \mathbf{u}^\top(t) \mathbf{R} \mathbf{u}(t) dt \quad (5.39)$$

where

$$\Psi(\mathbf{x}(t_f)) = \left\{ N^* - \sum_i [R^i(t_f) + V_+^i(t_f)] \right\}^2 \quad (5.40)$$

An equivalent form of the Bolza minimization problem can be formulated in

the Mayer form:

$$\hat{J}(\mathbf{x}(t), \mathbf{u}(t)) = \hat{\Psi}(\mathbf{x}(t_f)) \quad (5.41)$$

where

$$\hat{\Psi}(\mathbf{x}(t_f), \mathbf{u}) = \left\{ N^* - \sum_i [R^i(t_f) + V_+^i(t_f)] \right\}^2 + x_{eq}(t_f), \quad (5.42)$$

$$\dot{x}_{eq}(t) = f_{eq}(t, \mathbf{x}(t), \mathbf{u}(t)) = \sum_{i=1}^4 D^i(t) + \mathbf{u}^\top(t) \mathbf{R} \mathbf{u}(t) \quad (5.43)$$

From Lemma 5.3.1, it is inferred that the optimization problem has an optimal controller in the set of admissible controllers  $\tilde{U} \subset \mathbf{R}^{np}$ .

Also, define the adjoint variables or the costates,  $\mathbf{m}(t)$ , each component of which pertains to a system state. Let us denote each component of  $\mathbf{m}(t)$  as  $m_k^i(t)$ , for  $k \in \{S, E, I, R, D\}$  and  $m_k^{l,i}(t)$ , for  $k \in \{V_-, V_+\}$ .

As to ensure that  $S^i(t) \geq 0$ , the system state  $x_{sc}(t)$  must also be taken into account.

$$\bar{\mathbf{x}}(t) = [\mathbf{x}^\top(t) \quad x_{eq}(t) \quad x_{sc}(t)]^\top \quad (5.44)$$

$$\bar{\mathbf{m}}(t) = [\mathbf{m}^\top(t) \quad m_{eq}(t) \quad m_{sc}(t)]^\top \quad (5.45)$$

where  $x_{sc}(t)$  satisfies:

$$\begin{aligned} \dot{x}_{sc}(t) &= f_{sc}(t, \mathbf{x}(t), \mathbf{u}(t)) = \sum_i [S^i(t)]^2 \mathbb{1}(-S^i(t)), \\ x_{sc}(t_0) &= x_{sc}(t_f) = 0 \end{aligned} \quad (5.46)$$

The Hamiltonian function of the optimization problem is defined as:

$$\hat{H}(\mathbf{x}(t), \mathbf{u}(t), \mathbf{m}(t)) = \bar{\mathbf{m}}^\top(t) \mathbf{f}(t, \mathbf{x}(t), \mathbf{u}(t)) \quad (5.47)$$

where

$$\begin{aligned} \bar{\mathbf{m}}^\top(t) \mathbf{f}(t, \mathbf{x}, \mathbf{u}) &= \sum_i \left[ \sum_n m_n^i(t) f_n^i(t, \mathbf{x}, \mathbf{u}) + \sum_{\hat{n}} \sum_l m_{\hat{n}}^{l,i}(t) f_{\hat{n}}^{l,i}(t, \mathbf{x}, \mathbf{u}) \right] \\ &+ m_{sc}(t) f_{sc}(t, \mathbf{x}, \mathbf{u}) + m_{eq}(t) f_{eq}(t, \mathbf{x}, \mathbf{u}), \end{aligned} \quad (5.48)$$

for  $n \in \{S, E, I, R, D\}$ ,  $\hat{n} \in \{V_-, V_+\}$ .

From the adjoint final time conditions in Eq. (5.16), we have:

$$\begin{aligned} m_S^i(t_f) &= m_E^i(t_f) = m_I^i(t_f) = m_D^i(t_f) = m_{V_-}^{l,i}(t_f) = 0, \\ m_R^i(t_f) &= m_{V_+}^{l,i}(t_f) = -2 \left[ N^* - \sum_i (R^i(t_f) + V_+^i(t_f)) \right], \\ m_{\text{eq}}(t_f) &= 1 \end{aligned} \quad (5.49)$$

From the necessary condition in Eq. (5.17), we have:

$$\begin{aligned} -\dot{m}_S^i(t) &= -\lambda^i(t, \mathbf{I}(t))m_S^i(t) + \lambda^i(t, \mathbf{I}(t))m_E^i(t) + \frac{\partial f_{\text{sc}}^i}{\partial S^i}(t, \mathbf{x}(t), \mathbf{u}(t))m_{\text{sc}}(t) \\ -\dot{m}_E^i(t) &= -\sigma_i m_E^i(t) + \sigma_i m_I^i(t) \\ -\dot{m}_I^i(t) &= -\left[ \gamma_i + \eta_i(t) - \frac{a_{i,i}(t)}{N_i}(1 - v_{i,i}(t))S^i(t) \right] m_I^i(t) + \gamma_i m_R^i(t) + \eta_i(t)m_D^i(t) \\ -\dot{m}_R^i(t) &= -\xi_i m_R^i(t) + \xi_i m_S^i(t) \\ -\dot{m}_{V_-}^{l,i}(t) &= -\left[ \lambda^i(t, \mathbf{I}(t)) + \rho_l \frac{w_b^{l,i}}{\tau_l} \right] m_{V_-}^{l,i}(t) + \lambda^i(t, \mathbf{I}(t))m_E^i(t) + \rho_l \frac{w_b^{l,i}}{\tau_l} m_S^{l,i}(t) \\ -\dot{m}_{V_+}^{l,i}(t) &= -\psi_i m_{V_+}^{l,i}(t) + \psi_i m_S^i(t) \\ -\dot{m}_D^i(t) &= m_{\text{eq}}(t) \\ -\dot{m}_{\text{sc}}(t) &= 0 \\ -\dot{m}_{\text{eq}}(t) &= 0 \end{aligned} \quad (5.50)$$

It is important to notice that  $-\dot{m}_{\text{eq}}(t) = 0$  implies that  $m_{\text{eq}}(t) = c$  and since  $m_{\text{eq}}(t_f) = 1$ , then  $m_{\text{eq}}(t) = m_{\text{eq}} = 1$ . The time derivatives of costates remain the same as with the Bolza formulation of the minimization problem.

From the necessary condition in Eq. (5.19), the optimal control  $\mathbf{u}(t)$  with elements  $u^{l,i}(t)$  must satisfy:

$$\mathbf{u}^*(t) = \arg \min_{\mathbf{u}(t) \in \tilde{U}} H(\mathbf{x}(t), \mathbf{u}(t), \mathbf{m}(t)) \quad (5.51)$$

Let us now examine the Hessian matrix of the Hamiltonian function  $\hat{H}(\mathbf{x}, \mathbf{u}, \mathbf{m}(t))$ :

$$\frac{\partial^2 \hat{H}}{\partial \mathbf{u}^2}(\mathbf{x}(t), \mathbf{u}(t), \mathbf{m}(t)) = 2m_{\text{eq}} \begin{bmatrix} r_{1,1} & 0 & \dots & 0 \\ 0 & r_{2,2} & \dots & 0 \\ \vdots & \vdots & \ddots & 0 \\ 0 & 0 & \dots & r_{m,m} \end{bmatrix} = 2m_{\text{eq}} \mathbf{R} = 2\mathbf{R} > 0 \quad (5.52)$$

This indicates that  $\hat{H}(\mathbf{x}, \mathbf{u}, \mathbf{m}(t))$  is a strictly convex function.

Let us now define the indicator functions  $\phi^{l,i}(t)$  as before:

$$\phi^{l,i}(t) := \frac{1}{2} r_{\text{idx}, \text{idx}}^{-1} [m_{V_-}^{l,i}(t) - m_S^i(t)] \quad (5.53)$$

where  $\text{idx}$  denotes the row and column index of  $\mathbf{R}$  for the element that is the optimization weight of the control variable  $u^{l,i}(t)$  and is defined as:

$$\text{idx}(l, i) := 4(i - 1) + l \quad (5.54)$$

Given that the optimal solution exists and that it satisfies Eq. (5.51), we notice that the first derivative of the Hamiltonian is a linear function with respect to the control variable  $u^{l,i}(t)$ . Thus, the stationary point of the Hamiltonian is unique and therefore is a global minimum for the Hamiltonian.

The value for each control variable in  $\mathbf{u}(t)$  is then given by:

$$\begin{aligned} u^{l,i}(t) &= \max \{0, \min\{u_{\max}^{l,i}, \phi^{l,i}(t)\}\} \\ \iff u^{l,i}(t) &= \begin{cases} 0 & \phi^{l,i}(t) \leq 0 \\ \phi^{l,i}(t) & 0 \leq \phi^{l,i}(t) \leq u_{\max}^{l,i} \\ u_{\max}^{l,i} & u_{\max}^{l,i} \leq \phi^{l,i}(t) \end{cases} \end{aligned} \quad (5.55)$$

For the minimization problem given in the Mayer form, one can easily conclude that the controller which satisfies Pontryagin's conditions is the optimal controller under the assumption of convexity of the functional  $\mathbf{u} \mapsto \hat{\Psi}(\mathbf{x}(t_f, \mathbf{u}))$  in the control  $\mathbf{u}$ . The proof is given in Chapter 7 of [68]. This is indeed the case in our problem, since:

$$\frac{\partial^2 \hat{\Psi}}{\partial \mathbf{u}^2} = 2(t_f - t_0) \begin{bmatrix} r_{1,1} & 0 & \dots & 0 \\ 0 & r_{2,2} & \dots & 0 \\ \vdots & \vdots & \ddots & 0 \\ 0 & 0 & \dots & r_{m,m} \end{bmatrix} = 2(t_f - t_0) \mathbf{R} > 0 \quad (5.56)$$

Then, the elements  $u^{l,i}(t)$  of the optimal controller  $\mathbf{u}^*(t)$  are given by:

$$\begin{aligned} u_*^{l,i}(t) &= \max \{0, \min\{u_{\max}^{l,i}, \phi^{l,i}(t)\}\} \\ \iff u_*^{l,i}(t) &= \begin{cases} 0 & \phi^{l,i}(t) \leq 0 \\ \phi^{l,i}(t) & 0 \leq \phi^{l,i}(t) \leq u_{\max}^{l,i} \\ u_{\max}^{l,i} & u_{\max}^{l,i} \leq \phi^{l,i}(t) \end{cases} \end{aligned} \quad (5.57)$$

This completes the proof of the Theorem. □

Expressing the Bolza problem in the equivalent Mayer problem allows us to obtain the optimal controller given that  $\hat{\Psi}(\mathbf{x}(t_f, \mathbf{u}))$  is convex in the controls  $\mathbf{u}$ . In fact, any problem in the Bolza form can be expressed in the Mayer form using the methodology above. Therefore, the sufficiency of the convexity condition can be generalized to optimization problems in the Lagrange and the Bolza form.

# Chapter 6

## Conclusions And Future Work

### 6.1 Summary

The work presented in this thesis exhibits the preliminary steps required in order to develop the optimal control strategy upon a population in a pandemic. First, an epidemic model needs to be chosen in accordance with the various particularities of the disease in the population. Such particularities could include the latency from the exposure and the variability of the disease dynamics throughout the pandemic. This idea has been explored mainly in Chapter 1.

The system designer who wishes to model the outbreak of a disease might also have to consider what measurements can be taken from the system and how these could be expressed in terms of the system states. For the COVID-19 outbreak in Greece which has been considered throughout this work, this idea is elaborated in Chapter 2.

Chapter 3 discusses the main ways the designer can take into account in order to adequately identify the values of the system parameters.

In Chapter 4, the main results are presented for the COVID-19 outbreak in Greece. It can be seen that the model developed in this work in Chapter 1 can describe the progression of the pandemic effectively. An estimation for the true number of COVID-19 cases in Greece has also been proposed and the results were compared to other models. Using a-priori knowledge for the values of some of the system parameters and by utilizing it in the system identification, the values of the parameters were adequately described. Moreover, the relation between the fatality

rates and the NPI measures has been explored.

Chapter 5 provides the necessary background for Pontryagin's Minimum Principle. Existence of the optimal control policy for a vaccination strategy is proven and the necessary conditions for an optimal controller are given.

## 6.2 Future Work

Future expansions for the work presented here may include:

- Further differentiate the population by geolocation in order to model spatial heterogeneity of effective contacts.
- Further explore the idea of the application of Pontryagin's Principle for the outbreak of COVID-19 in Greece.

# Bibliography

- [1] Eric Bonabeau. «Agent-based modeling: Methods and techniques for simulating human systems». In: *Proceedings of the National Academy of Sciences* 99.suppl 3 (2002) (cit. on p. 1).
- [2] Eric Bonabeau. «Agent-based modeling: Methods and techniques for simulating human systems». In: *Proceedings of the National Academy of Sciences* 99 (2002), pp. 7280–7287 (cit. on p. 2).
- [3] Elizabeth Hunter, Brian Mac Namee, and John Kelleher. «An open-data-driven agent-based model to simulate infectious disease outbreaks». In: *PLOS ONE* 13 (2018). DOI: [10.1371/journal.pone.0208775](https://doi.org/10.1371/journal.pone.0208775) (cit. on p. 2).
- [4] W. O. Kermack and A. G. McKendrick. «A contribution to the mathematical theory of epidemics». In: *Proceedings of the Royal Society London A* 115 (1927) (cit. on pp. 2, 5).
- [5] Henry C. Tuckwell and Ruth J. Williams. «Some properties of a simple stochastic epidemic model of SIR type». In: *Mathematical Biosciences* 208 (2007). URL: <https://www.sciencedirect.com/science/article/pii/S002555640600188X> (cit. on p. 2).
- [6] Linda J.S. Allen. «A primer on stochastic epidemic models: Formulation, numerical simulation, and analysis». In: *Infectious Disease Modelling* 2 (2017) (cit. on p. 2).
- [7] S Lalwani et al. «Predicting optimal lockdown period with parametric approach using three-phase maturation SIRD model for COVID-19 pandemic». In: *Chaos, Solitons & Fractals* 138 (2020) (cit. on pp. 2, 5).
- [8] A D Ames et al. «Safety-Critical Control of Active Interventions for COVID-19 Mitigation». In: *Cold Spring Harbor Laboratory Press* 31 (2020) (cit. on pp. 2, 5).
- [9] A D Ames et al. «Safety-Critical Control of Compartmental Epidemiological Models with Measurement Delays». In: *Cold Spring Harbor Laboratory Press* 31 (2020) (cit. on pp. 2, 5).

- 
- [10] Wendi Wang. «Global behavior of an SEIRS epidemic model with time delays». In: *Applied Mathematics Letters* 15 (2002) (cit. on pp. 3, 5).
- [11] Min Chen et al. «The introduction of population migration to SEIAR for COVID-19 epidemic modeling with an efficient intervention strategy». In: *Information Fusion* 64 (2020) (cit. on pp. 3, 5).
- [12] Jin Jian-Min et al. «Gender Differences in Patients With COVID-19: Focus on Severity and Mortality». In: *Frontiers in Public Health* 8 (2020) (cit. on p. 3).
- [13] G. Wei-Jie et al. «Comorbidity and its impact on 1590 patients with COVID-19 in China: a nationwide analysis». In: *European Respiratory Journal* 57 (2020) (cit. on p. 3).
- [14] A. Clark et al. «Global, regional, and national estimates of the population at increased risk of severe COVID-19 due to underlying health conditions in 2020: a modelling study». In: *The Lancet Global Health* 8 (2020) (cit. on pp. 3, 8).
- [15] Gul Zaman, Yong Han Kang, and Il Hyo Jung. «Stability analysis and optimal vaccination of an SIR epidemic model». In: *Biosystems* 93.3 (2008), pp. 240–249 (cit. on p. 5).
- [16] Paolo Di Giamberardino and Daniela Iacoviello. «Optimal control of SIR epidemic model with state dependent switching cost index». In: *Biomedical Signal Processing and Control* 31 (2017) (cit. on p. 5).
- [17] E. Verriest, F. Delmotte, and M. Egerstedt. «Control of epidemics by vaccination». In: *Proceedings of the 2005, American Control Conference* 31 (2005) (cit. on p. 5).
- [18] Duccio Fanelli and Francesco Piazza. «Analysis and forecast of COVID-19 spreading in China, Italy and France». In: *Chaos, Solitons & Fractals* 134 (2020) (cit. on p. 5).
- [19] Takashi Odagaki. «Analysis of the outbreak of COVID-19 in Japan by SIQR model». In: *Infectious Disease Modelling* 5 (2020) (cit. on p. 5).
- [20] Mustafa Erdem, Muntaser Safan, and Carlos Castillo-Chavez. «Mathematical Analysis of an SIQR Influenza Model with Imperfect Quarantine». In: *Bulletin of Mathematical Biology* 79 (2017) (cit. on p. 5).
- [21] Michael Y. Li et al. «Global dynamics of a SEIR model with varying total population size». In: *Mathematical Biosciences* 160 (1999) (cit. on p. 5).
- [22] M. De la Sen and S. Alonso-Quesada. «Vaccination strategies based on feedback control techniques for a general SEIR-epidemic model». In: *Applied Mathematics and Computation* 218 (2011) (cit. on p. 5).
- [23] DF M Torres and A Rachah. «Analysis, Simulation and Optimal Control of a SEIR Model for Ebola Virus with Demographic Effects». In: *Communications Faculty Of Science Mathematics and Statistics* 67 (2018) (cit. on p. 5).

- 
- [24] Yukihiro Nakata and Toshikazu Kuniya. «Global dynamics of a class of SEIRS epidemic models in a periodic environment». In: *Journal of Mathematical Analysis and Applications* 363 (2010) (cit. on p. 5).
- [25] P. Mateus and Joaquim et al. «Optimal Control of Non-Autonomous SEIRS Models with Vaccination and Treatment». In: *Discrete & Continuous Dynamical Systems* 11 (2018) (cit. on p. 5).
- [26] B Ivorra et al. «Mathematical modeling of the spread of the coronavirus disease 2019 (COVID-19) taking into account the undetected infections. The case of China.» In: *Communications in nonlinear science & numerical simulation* 88 (2020) (cit. on p. 5).
- [27] H. Inaba. «Age-structured homogeneous epidemic systems with application to the MSEIR epidemic model». In: *Journal of Mathematical Biology* 54 (2007) (cit. on p. 5).
- [28] S. Zhao and H. Chen. «Modeling the epidemic dynamics and control of COVID-19 outbreak in China». In: *Quantitative Biology* 8 (2020) (cit. on p. 5).
- [29] A Abou-Ismaïl. «Compartmental Models of the COVID-19 Pandemic for Physicians and Physician-Scientists». In: *SN Comprehensive Clinical Medicine* 2 (2020) (cit. on p. 5).
- [30] Giordano, Giulia et al. «Modelling the COVID-19 Epidemic and Implementation of Population-Wide Interventions in Italy.» In: *Nature Medicine* 26 (2020) (cit. on p. 5).
- [31] M. Higazy. «Novel fractional order SIDARTHE mathematical model of COVID-19 pandemic.» In: *Chaos, Solitons & Fractals* 138 (2020) (cit. on p. 5).
- [32] F. Riccardo, M. Ajelli, X. Andrianou et al. «Epidemiological characteristics of COVID-19 cases in Italy and estimates of the reproductive numbers one month into the epidemic». In: *Preprint* (2020) (cit. on p. 8).
- [33] Zhou Fei et al. «Clinical course and risk factors for mortality of adult inpatients with COVID-19 in Wuhan, China: a retrospective cohort study». In: *The Lancet* 395 (2020) (cit. on p. 8).
- [34] Manash Pratim Barman et al. «COVID-19 pandemic and its recovery time of patients in India: A pilot study». In: *Diabetes & Metabolic Syndrome: Clinical Research & Reviews* 14 (2020) (cit. on p. 8).
- [35] TK. Kong. «Longer incubation period of coronavirus disease 2019 (COVID-19) in older adults». In: *Aging Med (Milton)* 3 (2020) (cit. on pp. 8, 23).
- [36] S. A. Lauer and K. H. Grantz and Q. Bi et al. «The Incubation Period of Coronavirus Disease 2019 (COVID-19) From Publicly Reported Confirmed Cases: Estimation and Application». In: *Ann Internal Medicine* 172 (2020) (cit. on pp. 8, 21).

- 
- [37] X. He, E.H.Y. Lau, and P. et al. Wu. «Temporal dynamics in viral shedding and transmissibility of COVID-19». In: *Nature Medicine* 26 (2020) (cit. on pp. 8, 23).
- [38] F. Javier Ibarondo et al. «Rapid Decay of Anti-SARS-CoV-2 Antibodies in Persons with Mild Covid-19». In: *New England Journal of Medicine* 383 (2020) (cit. on p. 8).
- [39] D. F. Gudbjartsson et al. «Humoral Immune Response to SARS-CoV-2 in Iceland». In: *New England Journal of Medicine* 383 (2020) (cit. on pp. 8, 23).
- [40] Helen Ward, Graham Cooke, and C. Atchison et al. «Declining prevalence of antibody positivity to SARS-CoV-2: a community study of 365,000 adults». In: *Preprint* (2020) (cit. on p. 8).
- [41] National Organization for Public Health of Greece. *Surveillance Data for COVID-19*. URL: <https://eody.gov.gr/epidimiologika-statistika-dedomena/ektheseis-covid-19/> (cit. on p. 12).
- [42] Johns Hopkins University (JHU). *COVID-19 Dashboard by the Center for Systems Science and Engineering (CSSE) at Johns Hopkins University (JHU)*. URL: <https://coronavirus.jhu.edu/map.html> (cit. on p. 12).
- [43] Johns Hopkins University (JHU). *COVID-19 Data Repository by the Center for Systems Science and Engineering (CSSE) at Johns Hopkins University*. URL: <https://github.com/CSSEGISandData/COVID-19> (cit. on p. 12).
- [44] Hellenic Government. *COVID-19 vaccination statistics*. URL: [https://data.gov.gr/datasets/mdg\\\_emvolio/](https://data.gov.gr/datasets/mdg\_emvolio/) (cit. on p. 12).
- [45] *COVID-19 Response Greece*. URL: <https://covid19response.gr/> (cit. on p. 12).
- [46] A. T. Levin, W. P. Hanage, N. Owusu-Boaitey, K. B. Cochran, S. P. Walsh G. Meyerowitz-Katz. *Assessing the age specificity of infection fatality rates for COVID-19: systematic review, meta-analysis, and public policy implications*. 2020 (cit. on p. 15).
- [47] K. M. Jagodnik, F. Ray, F. M. Giorgi, A. Lachmann. «Correcting under-reported COVID-19 case numbers: estimating the true scale of the pandemic». In: *Preprint* (2020) (cit. on p. 15).
- [48] M. Monod, A. Blenkinsop, X. Xi et al. «Age groups that sustain resurging COVID-19 epidemics in the United States». In: *Science Magazine* 371 (2021) (cit. on p. 15).
- [49] N. G. Davies, P. Klepac, Y. Liu et al. «Age-dependent effects in the transmission and control of COVID-19 epidemics». In: *Nature Medicine* 26 (2020) (cit. on p. 15).
- [50] National Organization for Public Health of Greece. *Press Conference regarding inoculation schedule 05/04/2021*. URL: <https://eody.gov.gr/enimerosi-20210405/> (cit. on pp. 16, 23).
-

- 
- [51] OECD, European Union. «Health at a Glance: Europe 2020: State of Health in the EU Cycle». In: *OECD Publishing, Paris* (2020) (cit. on p. 16).
- [52] V. Sypsa, S. Roussos, D. Paraskevis et al. «Modelling the SARS-CoV-2 first epidemic wave in Greece: social contact patterns for impact assessment and an exit strategy from social distancing measures». In: *Emerging Infectious Diseases* 27 (2021) (cit. on pp. 20, 22).
- [53] R. Verity, L. C. Okell et al. «Estimates of the severity of coronavirus disease 2019: a model-based analysis». In: *The Lancet Infectious Diseases* 20 (2020) (cit. on p. 21).
- [54] New York Times. *Coronavirus Vaccine Tracker*. URL: <https://www.nytimes.com/interactive/2020/science/coronavirus-vaccine-tracker.html> (cit. on pp. 21, 23).
- [55] Imperial College of London. *ICL Model*. URL: <https://mrc-ide.github.io/global-lmic-reports/> (cit. on p. 21).
- [56] P. G. T. Walker, C. Whittaker et al. «The impact of COVID-19 and strategies for mitigation and suppression in low- and middle-income countries». In: *Science Magazine* 369 (2020) (cit. on p. 22).
- [57] T. Ganyani, C. Kremer et al. «Estimating the generation interval for coronavirus disease (COVID-19) based on symptom onset data, March 2020». In: *Eurosurveillance* 25 (2020) (cit. on p. 22).
- [58] National Organization for Public Health of Greece, Hellenic Government. *Press Conference of 16/04/2021*. URL: <https://eody.gov.gr/enimerosi-20210416/> (cit. on p. 22).
- [59] S. Amit, G. Regev-Yochay, A. Afek et al. «Early rate reductions of SARS-CoV-2 infection and COVID-19 in BNT162b2 vaccine recipients». In: *The Lancet* 397 (2021) (cit. on p. 23).
- [60] U.S. Food and Drug Administration. *Fact Sheet for Healthcare Providers Administering Vaccine*. URL: <https://www.fda.gov/media/144413> (cit. on p. 23).
- [61] M. Voysey, S. A. Clemens et al. «Safety and efficacy of the ChAdOx1 nCoV-19 vaccine (AZD1222) against SARS-CoV-2: an interim analysis of four randomised controlled trials in Brazil, South Africa, and the UK». In: *The Lancet* 397 (2021) (cit. on p. 23).
- [62] D. G. Luenberger. *Introduction to Dynamic Systems: Theory, Models, and Applications*. New York: John Wiley Sons, 1979 (cit. on p. 49).
- [63] W. H. Fleming, R. W. Rishel. *Deterministic and stochastic optimal control*. Springer, 1975 (cit. on p. 53).
- [64] Hassan K Khalil. *Nonlinear systems; 3rd ed*. The book can be consulted by contacting: PH-AID: Wallet, Lionel. Upper Saddle River, NJ: Prentice-Hall, 2002. URL: <https://cds.cern.ch/record/1173048> (cit. on p. 54).
-

- [65] H. Schättler and U. Ledzewicz. *Optimal Control for Mathematical Models of Cancer Therapies: An Application of Geometric Methods*. New York-Heidelberg-Dordrecht-London: Springer, 2015 (cit. on p. 57).
- [66] K.R. Fister, S. Lenhart, and J.S. McNally. «Optimizing Chemotherapy in an HIV Model». In: *Electronic Journal of Differential Equations* 1998 (1998) (cit. on p. 57).
- [67] S.M. Lenhart and M.G. Bhat. «Application Of Distributed Parameter Control Model in Wildlife Damage Management». In: *Mathematical Models and Methods in Applied Sciences* 02 (1992) (cit. on p. 57).
- [68] Bressan, A., Piccoli, B. *Introduction to the Mathematical Theory of Control*. Amer Inst of Mathematical Sciences, 2007 (cit. on p. 61).